

RESULTS ON THE CKM ANGLE $\phi_1(\beta)$

T. E. BROWDER

*Department of Physics and Astronomy, University of Hawaii, 2505 Correa Road, Honolulu, HI 96822, USA
E-mail: teb@phys.hawaii.edu*

I review results related to the CKM angle $\phi_1(\beta)$. These results include recent measurements of CP -violation from the BaBar and Belle experiments in $b \rightarrow c\bar{c}s$, $b \rightarrow c\bar{c}d$ and $b \rightarrow s\bar{q}\bar{q}$ processes.

1 Introduction

1.1 The B Physics Program

The B physics program addresses several fundamental questions. Is the irreducible phase in the Cabibbo-Kobayashi-Maskawa (CKM) matrix the source of all CP -violating phenomena in the B system?¹ Or is CP -violation, the first manifestation of physics beyond the Standard Model? A related question is whether there are new CP -violating phases from physics beyond the Standard Model.²

The unitarity of the CKM matrix implies the existence of three measurable phases. In the convention favored at KEK and Belle, these are denoted

$$\phi_1 \equiv \arg \left(-\frac{V_{cd} V_{cb}^*}{V_{td} V_{tb}^*} \right) \quad (1)$$

$$\phi_2 \equiv \arg \left(-\frac{V_{ud} V_{ub}^*}{V_{td} V_{tb}^*} \right) \quad (2)$$

$$\phi_3 \equiv \arg \left(-\frac{V_{cd} V_{cb}^*}{V_{ud} V_{ub}^*} \right). \quad (3)$$

while at SLAC and at BaBar these angles are usually referred to as β , α and γ , respectively.

As first noted by Bigi, Carter and Sanda,³ there are large measurable CP -asymmetries in the decays of neutral B mesons to CP -eigenstates. In the decay chain $\Upsilon(4S) \rightarrow B^0 \bar{B}^0 \rightarrow f_{CP} f_{tag}$, where one of the B mesons decays at time t_{CP} to a final state f_{CP} and the other decays at time t_{tag} to a final state f_{tag} that distinguishes between B^0 and \bar{B}^0 , the decay rate has a time dependence given by³

$$\frac{e^{-\frac{|\Delta t|}{\tau_{B^0}}}}{4\tau_{B^0}} \left\{ 1 + q \cdot [\mathcal{S} \sin(\Delta m_d \Delta t) + \mathcal{A} \cos(\Delta m_d \Delta t)] \right\},$$

where τ_{B^0} is the B^0 lifetime, Δm_d is the mass difference between the two B^0 mass eigenstates, $\Delta t = t_{CP} - t_{tag}$, and the b -flavor charge $q = +1$ (-1) when the tagging B meson is a B^0 (\bar{B}^0). The CP -violation

parameters \mathcal{S} and \mathcal{A} are given by

$$\mathcal{S} \equiv \frac{2\mathcal{I}m(\lambda)}{|\lambda|^2 + 1}, \quad \mathcal{A} \equiv \frac{|\lambda|^2 - 1}{|\lambda|^2 + 1}, \quad (4)$$

where λ is a complex parameter that depends on both the $B^0 \bar{B}^0$ mixing and on the amplitudes for B^0 and \bar{B}^0 to decay to f_{CP} . To a good approximation, the SM predicts $\mathcal{S} = -\xi_f \sin 2\phi_1$, where $\xi_f = +1(-1)$ corresponds to CP -even (-odd) final states. Direct CP -violation, $\mathcal{A} = 0$ (or equivalently $|\lambda| = 1$), is expected for both $b \rightarrow c\bar{c}s$ and $b \rightarrow s\bar{s}s$ transitions.

1.2 Accelerators and Detectors

The B -factory accelerators, PEP-II⁴ and KEKB⁵ were commissioned with remarkable speed starting in late 1998. The experiments, BaBar⁶ and Belle,⁷ started physics data taking in 1999. In the summer of 2001, the two experiments announced the observation of the first statistically significant signals for CP -violation outside of the kaon system.^{8,9}

Due to the extraordinary performance of the two accelerators, the most recent results reported in the summer of 2003 at the Lepton-Photon Symposium are based on very large data samples. BaBar has integrated 113 fb^{-1} on the $\Upsilon(4S)$ resonance while Belle has integrated a sample of 140 fb^{-1} . KEK-B also passed a critical milestone for e^+e^- storage rings and achieved a peak luminosity above $1 \times 10^{34} \text{ cm}^{-2}\text{s}^{-1}$.

1.3 The Principle of the Measurement

The measurement of time-dependent CP -asymmetry requires:

- A large sample of $\Upsilon(4S)$ decays into $B^0 \bar{B}^0$ pairs. To boost the $\Upsilon(4S)$ decay frame so that the B mesons' flight length can be measured with solid-state vertex detector technology, both the KEKB and PEP-II accelerators use asymmetric energy beams with energies of 8.0 and 3.5 GeV or 9.0 and 3.1 GeV, respectively.

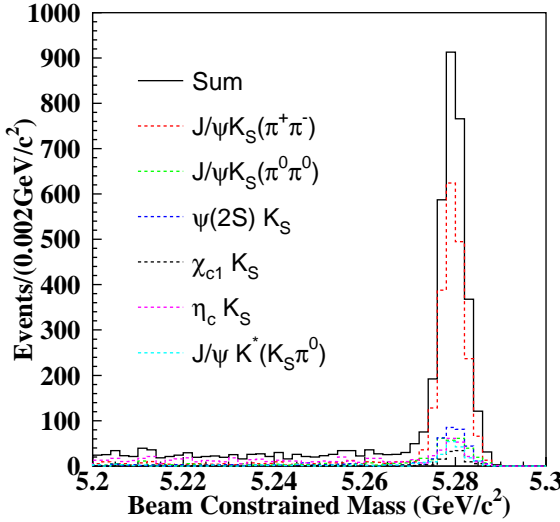


Figure 1. The fully reconstructed CP -eigenstate sample used by Belle. This sample is obtained from a data sample with an integrated luminosity of 140 fb^{-1} .

- Efficient reconstruction of $B \rightarrow X_{cc}K^0$ decays. This implies accurate measurements of momenta and energies of neutrals using CsI(Tl) crystal calorimeters in addition to good charged particle tracking in small cell drift chambers and efficient identification of leptons and K_S^0 as well as K_L^0 mesons.
- A measurement of Δt . This is related to the measurement of Δz , the spatial distance between the decay vertices and achieved at both experiments by using double-sided silicon strip detectors situated at small radii close to the interaction point.
- A determination of the flavor of the accompanying B (“tagging”); this is based on the identification of electrons, muons and charged kaons and the measurement of their charge.

More detailed descriptions of the detectors^{6,7} and the experimental analysis procedure are available elsewhere.¹⁰

2 Status of CP -Violation in $b \rightarrow c\bar{c}s$ Processes

Belle and BaBar reconstruct B^0 decays to the following $b \rightarrow c\bar{c}s$ CP -eigenstates: $J/\psi K_S$, $\psi(2S)K_S$,

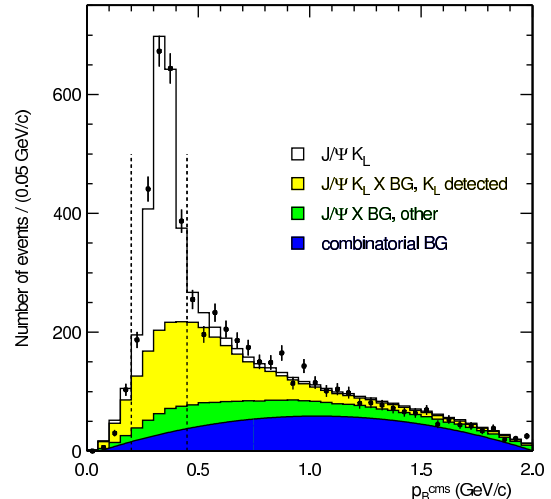


Figure 2. The p_B^* (B momentum in the CM frame) distribution for the $B \rightarrow J/\psi K_L$ sample used by Belle. This sample is obtained from a data sample with an integrated luminosity of 140 fb^{-1} . The shaded portions show the contributions of different background components. The vertical dashed lines indicate the signal region.

$\chi_{c1}K_S$, η_cK_S for $\xi_f = -1$ and $J/\psi K_L$ for $\xi_f = +1$.¹¹ The two classes ($\xi_f = \pm 1$) should have CP -asymmetries that are opposite in sign.

Both experiments also use $B^0 \rightarrow J/\psi K^{*0}$ decays where $K^{*0} \rightarrow K_S\pi^0$. Here the final state is a mixture of even and odd CP . The CP content can, however, be determined from an angular analysis of other ψK^* decays. The CP -odd fraction is found to be small (i.e. $(19 \pm 4)\%$ ($(16 \pm 3.5)\%$) in the Belle (BaBar) analysis).

The most recent BaBar analysis is based on a data sample with an integrated luminosity of 81 fb^{-1} and was first presented in 2002.⁹ There is a corresponding published Belle result also shown in 2002 with 78 fb^{-1} .⁸ At this Symposium, Belle provided a new preliminary result for their 140 fb^{-1} sample.¹²

The data sample used for the recent Belle measurement is shown in Fig. 1 and Fig. 2. Table 1 lists the numbers of candidates, N_{ev} , and the estimated signal purity for each f_{CP} mode. It is clear that the CP -eigenstate samples that are used for the CP -violation measurements in $b \rightarrow c\bar{c}s$ are large and clean.

In the summer of 2001, the first statistically significant measurements of the CP -violating parameter $\sin 2\phi_1$ were reported by Belle and BaBar. Belle

Table 1. The yields from Belle for reconstructed $B \rightarrow f_{CP}$ candidates after flavor tagging and vertex reconstruction, N_{ev} , and the estimated signal purity, p , in the signal region for each f_{CP} mode. J/ψ mesons are reconstructed in $J/\psi \rightarrow \mu^+\mu^-$ or e^+e^- decays. Candidate K_S^0 mesons are reconstructed in $K_S^0 \rightarrow \pi^+\pi^-$ decays unless otherwise written explicitly.

Mode	ξ_f	N_{ev}	p
$J/\psi K_S^0$	-1	1997	0.976 ± 0.001
$J/\psi K_S^0(\pi^0\pi^0)$	-1	288	0.82 ± 0.02
$\psi(2S)(\ell^+\ell^-)K_S^0$	-1	145	0.93 ± 0.01
$\psi(2S)(J/\psi\pi^+\pi^-)K_S^0$	-1	163	0.88 ± 0.01
$\chi_{c1}(J/\psi\gamma)K_S^0$	-1	101	0.92 ± 0.01
$\eta_c(K_S^0 K^- \pi^+)K_S^0$	-1	123	0.72 ± 0.03
$\eta_c(K^+ K^- \pi^0)K_S^0$	-1	74	0.70 ± 0.04
$\eta_c(p\bar{p})K_S^0$	-1	20	0.91 ± 0.02
All with $\xi_f = -1$	-1	2911	0.933 ± 0.002
$J/\psi K^{*0}(K_S^0\pi^0)$	+1(81%)	174	0.93 ± 0.01
$J/\psi K_L^0$	+1	2332	0.60 ± 0.03

found

$$\sin 2\phi_1 = 0.99 \pm 0.14 \pm 0.06 \quad (5)$$

while BaBar obtained

$$\sin 2\phi_1 = 0.59 \pm 0.14 \pm 0.05. \quad (6)$$

The results were based on data samples of comparable size (31 million and 32 million $B\bar{B}$ pairs, respectively).

The new Belle data are shown in Fig. 3. This figure shows the Δt distributions where a clear shift between B^0 and \bar{B}^0 tags is visible as well as the raw asymmetry plots in two bins of the flavor tagging quality variable r . For low-quality tags ($0 < r < 0.5$), which have a large background dilution, only a modest asymmetry is visible while in the subsample with high quality tags ($0.5 < r < 1.0$), a very clear asymmetry with a sine-like time modulation is present. The final results are extracted from an unbinned maximum-likelihood fit to the Δt distributions that takes into account resolution, mistagging and background dilution. The new Belle result with 140 fb^{-1} (152 million $B\bar{B}$ pairs) is

$$\sin 2\phi_1 = 0.733 \pm 0.057 \pm 0.028. \quad (7)$$

The new Belle result may be compared to the BaBar result with 78 fb^{-1} of

$$\sin 2\phi_1 = 0.741 \pm 0.067 \pm 0.03. \quad (8)$$

Both experiments are now in very good agreement. A new world average can be calculated from these results,

$$\sin 2\phi_1 = 0.736 \pm 0.049. \quad (9)$$

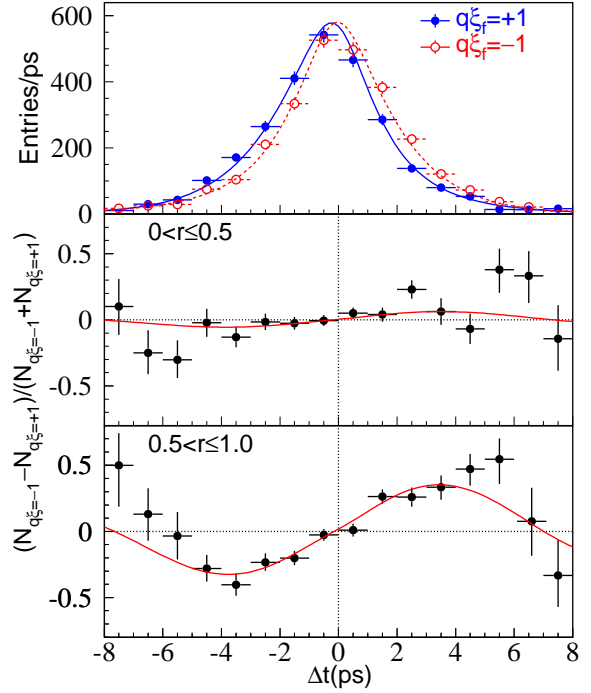


Figure 3. Belle data from 2003: (a) Δt distributions for B^0 and \bar{B}^0 tags (b) raw asymmetry for low-quality tags and (c) raw asymmetry for high-quality tags. The smooth curves are projections of the unbinned likelihood fit.

This world average can be interpreted as a constraint on the CKM angle ϕ_1 . This constraint can be compared to the indirect determinations on the unitarity triangle.¹³ This comparison is shown in Fig. 4 and is consistent with the hypothesis that the Kobayashi-Maskawa phase is the source of CP -violation.

The measurement of $\sin(2\phi_1)$ in $b \rightarrow c\bar{c}s$ modes, although still statistically limited, is becoming a precision measurement. The systematics are small and well-understood. Recently, BaBar physicists discovered a new small source of systematic uncertainty due to CP -violation in $b \rightarrow c\bar{u}d$ decays on the tagging side.¹⁴

The presence of an asymmetry with a cosine dependence ($|\lambda| \neq 1$) would indicate direct CP -violation. In order to test for this possibility in $b \rightarrow c\bar{c}s$ modes, Belle also performed a fit with $a_{CP} \equiv -\xi_f \text{Im}\lambda/|\lambda|$ and $|\lambda|$ as free parameters, keeping everything else the same. They obtain

$$|\lambda| = 1.007 \pm 0.041(\text{stat}) \quad (10)$$

$$a_{CP} = 0.733 \pm 0.057(\text{stat}),$$

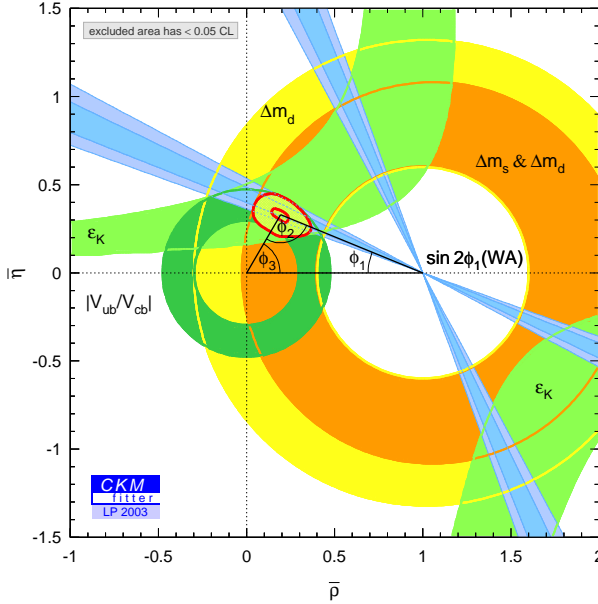


Figure 4. Indirect constraints on the angles of the CKM triangle compared to the most recent direct measurements of ϕ_1 from Belle and BaBar. The theoretical uncertainties in the indirect constraints are conservatively estimated by the CKM fitter group.

for all the $b \rightarrow c\bar{s}s$ CP modes combined. This result is consistent with the assumption used in their primary analysis.

3 Studies of CP -Violation in $b \rightarrow c\bar{d}$ Processes

Neutral B decays to CP -eigenstates that proceed by $b \rightarrow c\bar{d}$ processes are expected to have the same CP -violation as $b \rightarrow c\bar{s}s$ since both are sensitive to the phase of $B - \bar{B}$ mixing. A small deviation from this expectation is possible because of the contribution of $b \rightarrow d$ penguin diagrams (a.k.a. “penguin pollution”) in the decay modes that are examined. Penguin pollution may also give rise to direct CP -violation and a CP -violating term with a $\cos(\Delta m_d \Delta t)$ dependence.

The $b \rightarrow c\bar{d}$ decay modes that have been used so far for CP -violation studies are $B \rightarrow D^{*+}D^{*-}$, $B \rightarrow D^{*+}D^-$, and $B \rightarrow J/\psi\pi^0$.¹⁵⁻¹⁸ The effect of penguin pollution might be expected to be the largest in $B \rightarrow J/\psi\pi^0$ because the penguin contribution is not color-suppressed in that mode.

For $B \rightarrow \psi\pi^0$, with 81 fb^{-1} BaBar has a signal of 40 ± 7 events¹⁵ and finds

$$\sin 2\phi_{1eff}(B \rightarrow \psi\pi^0) = 0.05 \pm 0.45 \pm 0.16. \quad (11)$$

The corresponding result from Belle is based on 140 fb^{-1} and uses 89 ± 10 events.¹⁶ They obtain

$$\sin 2\phi_{1eff}(B \rightarrow \psi\pi^0) = 0.72^{+0.37}_{-0.42} \pm 0.08. \quad (12)$$

In both cases, the systematic error includes the possibility of CP -violation in a small component of the background that peaks under the signal.

The $b \rightarrow c\bar{d}$ mode $B \rightarrow D^{*+}D^{*-}$ has a vector-vector final state and requires special treatment since it includes contributions from both CP -even and odd components. To extract the CP -odd fraction, one fits the angular distribution in the transversity basis. The result from BaBar based on a sample with 156 ± 14 signal events is,

$$R_\perp = 0.063 \pm 0.055 \pm 0.009, \quad (13)$$

where the quantity R_\perp is the fraction of the CP -odd component. The measurement indicates that $B^0 \rightarrow D^{*+}D^{*-}$ is mostly CP -even.

The time distributions from BaBar for $B \rightarrow D^{*+}D^{*-}$ are shown in Fig. 5. BaBar finds

$$\sin 2\phi_{1eff}(B \rightarrow D^{*+}D^{*-}) = -0.05 \pm 0.29 \pm 0.10, \quad (14)$$

which is about 2.5σ from the result in $b \rightarrow c\bar{s}s$ modes. This may be a statistical fluctuation or could be an indication that the Standard Model $b \rightarrow d$ penguin contribution is large. The fit includes the possibility of direct CP -violation. The parameter λ is found to be $0.75 \pm 0.19 \pm 0.02$, which is consistent with unity, as expected for no direct CP -violation.

Since $B^0 \rightarrow D^{*+}D^-$ and its charge conjugate are not CP -eigenstates, a modified treatment is required. There are four rather than two CP -violating observables that are determined from a time-dependent fit to the different D^*D charge states.

BaBar finds,

$$S_{+-} = -0.82 \pm 0.75 \pm 0.14, \quad (15)$$

$$S_{-+} = -0.24 \pm 0.69 \pm 0.12, \quad (16)$$

$$A_{+-} = +0.47 \pm 0.40 \pm 0.12, \quad (17)$$

$$A_{-+} = +0.22 \pm 0.37 \pm 0.10. \quad (18)$$

In the limit of no penguins and assuming factorization in these hadronic decays, $S_{-+} = S_{+-} = -\sin 2\phi_1$ and $A_{+-} = A_{-+} = 0$. The above results for CPV in $B \rightarrow D^*D$ decays are consistent with this limit.

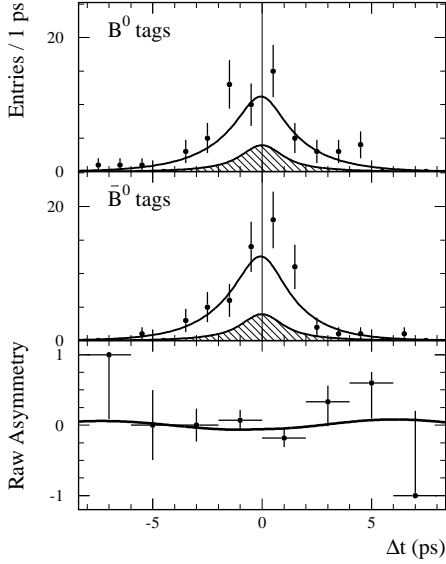


Figure 5. BaBar results on CP -violation in $B \rightarrow D^{*+}D^{*-}$. The top two figures show the Δt distributions for B^0 and \bar{B}^0 tags. The third plot shows the raw time asymmetry distribution.

Observation of the CP -eigenstate mode $B \rightarrow D^+D^-$ was reported by Belle at this conference. With 140 fb^{-1} , the 5σ signal contains 24.3 ± 6.0 events. In the future, this mode can also be used for time-dependent measurements of CPV in $b \rightarrow c\bar{c}d$ processes.

The results of CP -violation measurements for $b \rightarrow c\bar{c}d$ decays are summarized in Fig. 6. The measurements are not yet precise enough to definitively demonstrate the presence of penguin pollution.

4 Status of CP -Violation in $b \rightarrow sq\bar{q}$ Penguin Processes

In addition to the program of measuring the other remaining angles of the unitarity triangle that is discussed in the contribution by Jawahery,¹⁹ there is also the question of whether there are additional CP -violating phases from new interactions or physics beyond the Standard Model. At the moment, such new phases are poorly constrained.

One way to attack this question is to measure the time-dependent CP -asymmetry in penguin-dominated modes such as $B^0 \rightarrow \phi K_S^0$, $B^0 \rightarrow \eta' K_S^0$ or $B^0 \rightarrow K_S^0 \pi^0$, where heavy new particles may contribute inside the loop, and compare it to the asymmetry in $B^0 \rightarrow J/\psi K_S^0$ and related $b \rightarrow c\bar{c}s$ charmonium modes.

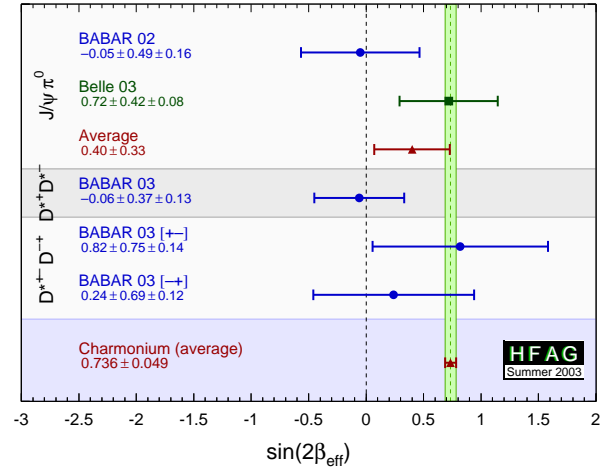


Figure 6. Summary plot of results on CP -violation in $b \rightarrow c\bar{c}d$ modes.

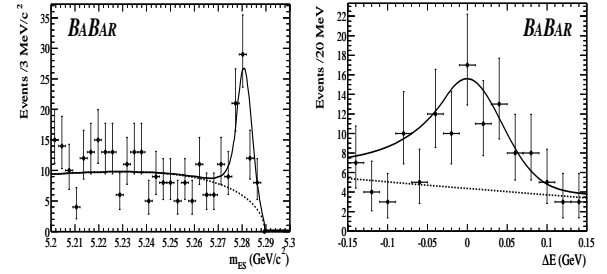


Figure 7. Beam constrained mass and ΔE distributions for $B \rightarrow K_S^0 \pi^0$ from BaBar.

The mode $B \rightarrow K_S \pi^0$ proceeds through a $b \rightarrow s\bar{d}\bar{d}$ transition. The BaBar data on $B \rightarrow K_S^0 \pi^0$ are shown in Fig. 7. To be useful for time-dependent CPV studies at least one of charged pions from the K_S^0 must be detected in the BaBar silicon vertex detector.²⁰ There are 123 ± 16 events of this type that are then used to obtain

$$\sin 2\phi_{1\text{eff}}(B \rightarrow K_S^0 \pi^0) = 0.48^{+0.38}_{-0.47} \pm 0.11. \quad (19)$$

The time distributions are shown in Fig. 8. The direct CP -violation parameter is $A = -0.40^{+0.28}_{-0.27} \pm 0.10$.²⁰ When A is fixed to zero, the value of $S = \sin(2\phi_{1\text{eff}})$ shifts slightly to $0.41^{+0.41}_{-0.48} \pm 0.11$. The results for $B \rightarrow K_S \pi^0$ are consistent with the value from the $b \rightarrow c\bar{c}s$ modes, $\sin 2\phi_1 = 0.736 \pm 0.049$.

The mode $B \rightarrow \eta' K_S^0$ is expected to include contributions from $b \rightarrow s\bar{u}\bar{u}$ and $b \rightarrow s\bar{d}\bar{d}$ penguin processes. The beam constrained mass distribution for the $B \rightarrow \eta' K_S^0$ sample used by Belle is shown in

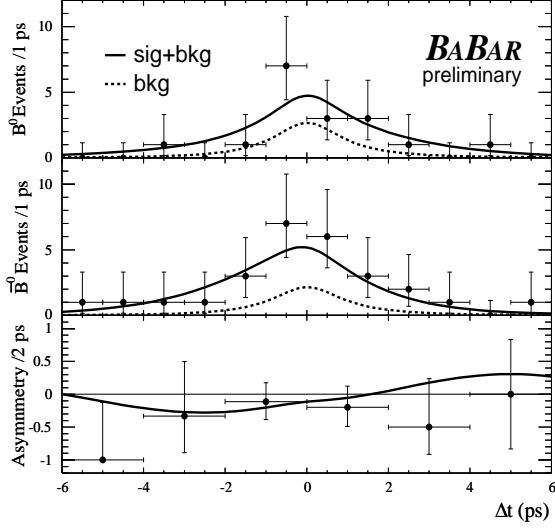


Figure 8. BaBar data on $B \rightarrow K_S^0 \pi^0$. The top two figures show the Δt distributions for B^0 and \bar{B}^0 tags, separately. The third plot shows the raw time asymmetry distribution.

Fig. 9 and contains 244 ± 21 signal events.²¹ Belle finds (Fig. 10),

$$\sin 2\phi_{1eff}(B \rightarrow \eta' K_S^0) = 0.43 \pm 0.27 \pm 0.05 \quad (20)$$

The BaBar data is shown in Fig. 11. They obtain,

$$\sin 2\phi_{1eff}(B \rightarrow \eta' K_S^0) = 0.02 \pm 0.34 \pm 0.03 \quad (21)$$

The average of these two results for $B \rightarrow \eta' K_S^0$ is about 2.2σ from the $b \rightarrow c\bar{s}s$ measurement, which is the Standard Model expectation.

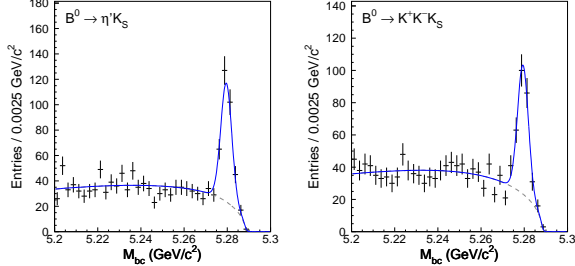


Figure 9. Beam constrained mass distributions for $B \rightarrow \eta' K_S^0$ (left) and $B \rightarrow K^+ K^- K_S^0$ (right).

The decay mode $B \rightarrow K^+ K^- K_S^0$, where $K^+ K^-$ combinations consistent with the ϕ have been removed, is found by Belle to be dominantly CP -odd²² and thus can be treated as a CP -eigenstate and used for studies of time-dependent CP -violation in

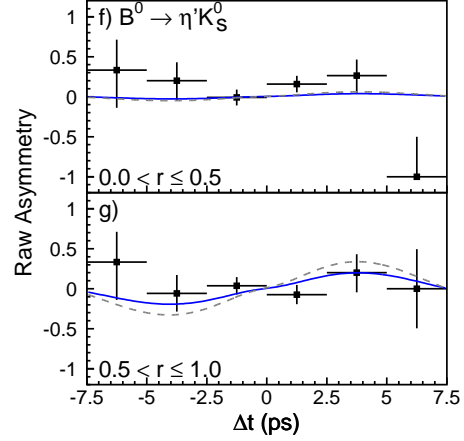


Figure 10. Belle data for the raw asymmetry in $B^0 \rightarrow \eta' K_S^0$. The upper plot shows the data for low-quality tags while the lower plot shows the higher quality tags. The dashed curves are the expectations from the Standard Model.

$b \rightarrow sq\bar{q}$ processes. The beam constrained mass distribution for the $B \rightarrow K^+ K^- K_S^0$ sample used by Belle is shown in Fig. 9. There are 199 ± 18 signal events. Belle obtains,

$$\sin 2\phi_{1eff}(B \rightarrow K^+ K^- K_S^0) = 0.51 \pm 0.26 \pm 0.05^{+0.18}_{-0.00}, \quad (22)$$

where the third error is due to the uncertainty in the CP content of this final state.²² The results for $B \rightarrow K^+ K^- K_S^0$ are also consistent with $b \rightarrow c\bar{s}s$ decays. However, in this decay there is also the possibility of ‘‘tree-pollution’’, the contribution of the $b \rightarrow u\bar{u}s$ tree amplitude that may complicate the interpretation of the results.²³

The $B^0 \rightarrow \phi K_S^0$ decay, which is dominated by the $b \rightarrow s\bar{s}s$ transition, is an especially unambiguous and sensitive probe of new CP -violating phases from physics beyond the SM.²⁴ The SM predicts that measurements of CP -violation in this mode should yield $\sin 2\phi_1$ to a very good approximation.^{25,23} A significant deviation in the time-dependent CP -asymmetry in this mode from what is observed in $b \rightarrow c\bar{s}s$ decays would be evidence for a new CP -violating phase.

The $B \rightarrow \phi K_S^0$ sample used by BaBar is shown in Fig. 12. The signal, obtained from a sample with an integrated luminosity of 110 fb^{-1} , contains 70 ± 9 events.²⁰ The time distributions for the BaBar data are shown in Fig. 13. They obtain

$$\sin 2\phi_{1eff}(B \rightarrow \phi K_S^0) = 0.45 \pm 0.43 \pm 0.07. \quad (23)$$

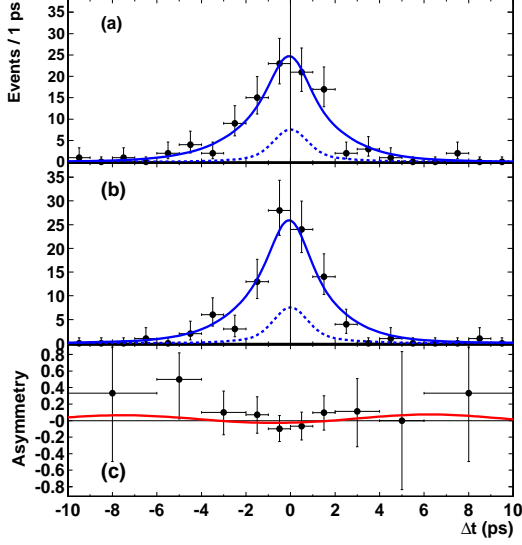


Figure 11. BaBar data on $B \rightarrow \eta' K_S^0$. The top two figures show the Δt distributions for B^0 and \bar{B}^0 tags, separately. The third plot shows the raw time asymmetry distribution.

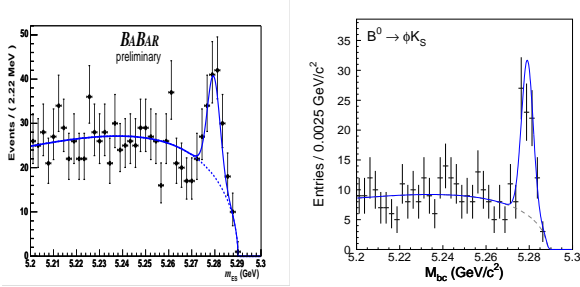


Figure 12. Beam constrained mass distributions for $B \rightarrow \phi K_S^0$ from BaBar (left) and Belle (right).

This value is consistent with the Standard Model expectation, but is somewhat different from the value obtained with the 81 fb^{-1} sample, which was $\sin 2\phi_{1\text{eff}} = -0.18 \pm 0.51 \pm 0.09$. The new result includes more data and a reprocessing of the old data sample. After extensive checks with data and Toy Monte Carlo studies, the large change in the central value is attributed to a 1σ statistical fluctuation.²⁶

The $B \rightarrow \phi K_S^0$ sample used by Belle is shown in the right panel of Fig. 12. The selection criteria are described in detail elsewhere.^{27,28} The signal contains 68 ± 11 events. Figure 15 shows the raw asymmetries from Belle in two regions of the flavor-tagging parameter r . While the numbers of events in the two regions are similar, the effective tagging efficiency is

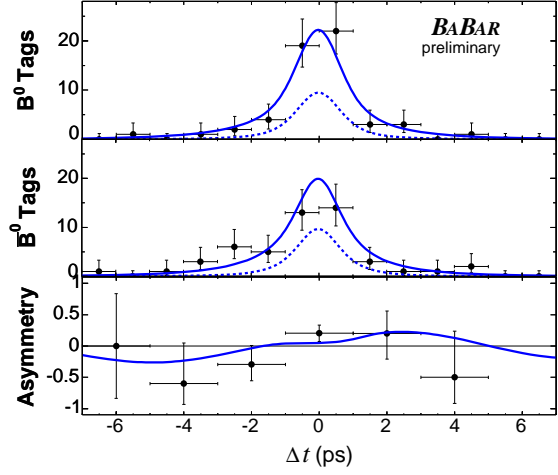


Figure 13. BaBar time difference and asymmetry data distributions in $B \rightarrow \phi K_S^0$. The top two figures show the Δt distributions for B^0 and \bar{B}^0 tags, separately. The third plot shows the raw time asymmetry distribution.

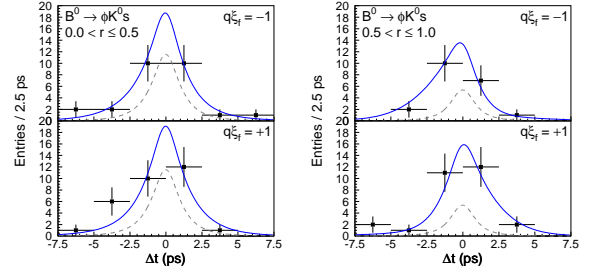


Figure 14. Belle data: (left) Δt distributions for low-quality tags and (right) for high-quality tags. The dashed curves show the background contributions.

much larger and the background dilution is smaller in the region $0.5 < r \leq 1.0$. The solid curves show the results of the unbinned maximum-likelihood fit to the Δt distribution.

The observed CP -asymmetry for $B^0 \rightarrow \phi K_S^0$ in the region $0.5 < r \leq 1.0$ (Fig. 15 (lower panel)) indicates the difference from the SM expectation (dashed curve). Note that these projections onto the Δt axis do not take into account event-by-event information (such as the signal fraction, the wrong tag fraction and the vertex resolution) that is used in the unbinned maximum likelihood fit.

The contamination of $K^+ K^- K_S^0$ events in the ϕK_S^0 sample ($7.2 \pm 1.7\%$) is small. Finally, backgrounds from the $B^0 \rightarrow f_0(980) K_S^0$ decay, which has the opposite CP -eigenvalue to ϕK_S^0 , are found to be

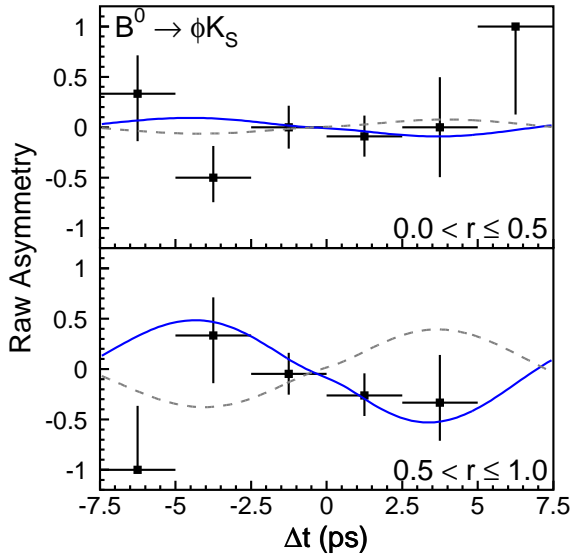


Figure 15. Belle data for the raw asymmetry in $B^0 \rightarrow \phi K_S^0$. The upper plot shows the data for low-quality tags while the lower plot shows the higher quality tags. The dashed line is the expectation from the Standard Model.

small ($1.6^{+1.9\%}_{-1.5\%}$). The influence of these backgrounds is treated as a source of systematic uncertainty.

Belle obtains

$$\sin 2\phi_{1\text{eff}}(B \rightarrow \phi K_S^0) = -0.96 \pm 0.5^{+0.09}_{-0.11} \quad (24)$$

from their likelihood fit to the ϕK_S^0 data. The likelihood function is parabolic and well-behaved. An evaluation of the significance of the result using the Feldman-Cousins method and allowing for systematic uncertainties shows that this result deviates by 3.5σ from the Standard Model expectation.²⁸

The Belle group performed a number of validation checks for their $B \rightarrow \phi K_S^0$ CP -violation result. Fits to the same samples with the direct CP -violation parameter \mathcal{A} fixed at zero yield $\sin 2\phi_{1\text{eff}} = -0.99 \pm 0.50(\text{stat})$ for $B^0 \rightarrow \phi K_S^0$. As a consistency check for the \mathcal{S} term, the same fit procedure is applied to the charged B meson decays $B^+ \rightarrow \phi K^+$. The result is $\mathcal{S} = -0.09 \pm 0.26(\text{stat})$, $\mathcal{A} = +0.18 \pm 0.20(\text{stat})$ for $B^+ \rightarrow \phi K^+$ decay. The results for the \mathcal{S} term is consistent with no CP -asymmetry, as expected. The asymmetry distribution is shown in Fig. 16. In addition, the ϕK_S^0 sideband has been examined as shown in Fig. 16. No asymmetry is found in that sample.

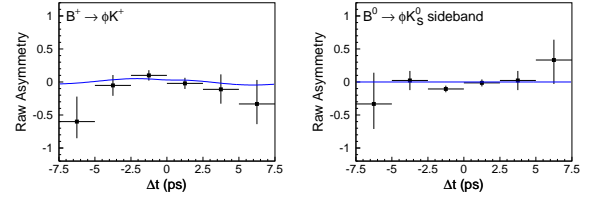


Figure 16. Belle data: consistency checks of the $B \rightarrow \phi K_S^0$ analysis. The asymmetries in (a) the $B^\pm \rightarrow \phi K^\pm$ sample and (b) the $B \rightarrow \phi K_S^0$ sideband sample.

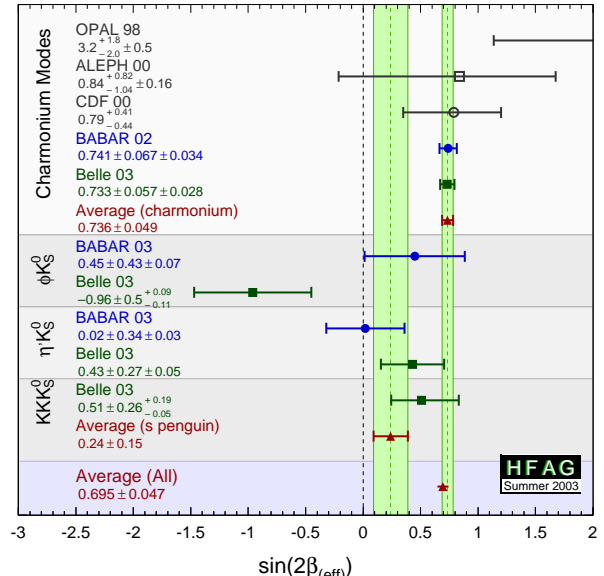


Figure 17. Summary plot of results on $\sin 2\phi_1$ and $\sin 2\phi_{1\text{eff}}$ in $b \rightarrow c\bar{s}s$ and $b \rightarrow s\bar{q}q$ modes.

5 Conclusion

Belle presented a new measurement of time-dependent CP -violation in $b \rightarrow c\bar{s}s$ CP -eigenstates. This result and previous results from BaBar are in good agreement with each other and with the hypothesis that the Kobayashi-Maskawa phase is the source of CP -violation.

Studies of CP -violation in $b \rightarrow c\bar{c}d$ modes are progressing. In $B \rightarrow D^{*+}D^{*-}$ decays, BaBar observes a 2.5σ hint for penguin pollution. More data and measurements are needed to clarify whether penguin pollution is present in this class of decays.

In $B \rightarrow \phi K_S^0$ decays there was a surprise. With 140 fb^{-1} Belle observed a 3.5σ deviation from the Standard Model expectation. This could be an indication of new physics from heavy particles in the

$b \rightarrow s\bar{s}$ penguin loop. However, BaBar's value moved closer to the Standard Model with the addition of new data and reprocessing. More precise measurements of the other $b \rightarrow sq\bar{q}$ modes can further constrain phases from new physics. For example, new physics may contribute differently to pseudoscalar-vector and pseudoscalar-pseudoscalar modes.²

The results of CP -violation measurements for $b \rightarrow sq\bar{q}$ penguin decays are summarized in Fig. 17. The world average for all $b \rightarrow s$ penguin decays (shown by the dotted line) appears to be displaced from the average for $b \rightarrow c\bar{c}s$ modes. The high energy physics community will require that this experimental issue be resolved conclusively in the future. This will require large data samples with integrated luminosities of at least 1 ab^{-1} or 1000 fb^{-1} .

Acknowledgments

I thank Harry Cheung for his patience and Andreas Hoecker for his contributions to the figures. I also wish to thank my colleagues at KEK-B, PEP-II, Belle and BaBar for their extraordinary contributions to the work reported here.

References

1. M. Kobayashi and T. Maskawa, *Prog. Theor. Phys.* **49**, 652 (1973).
2. Y. Grossman, contributions to these proceedings.
3. A. B. Carter and A. I. Sanda, *Phys. Rev. D* **23**, 1567 (1981); I. I. Bigi and A. I. Sanda, *Nucl. Phys.* **B193**, 85 (1981).
4. "PEP-II: An asymmetric B Factory", Conceptual Design Report, SLAC-418, LBL-5379 (1993).
5. S. Kurokawa and E. Kikutani *et al.*, *Nucl. Instrum. Methods A* **499**, 1 (2003).
6. Belle Collaboration, A. Palano *et al.*, *Nucl. Instrum. Methods A* **479**, 1 (2002).
7. Belle Collaboration, A. Abashian *et al.*, *Nucl. Instrum. Methods A* **479**, 117 (2002).
8. Belle Collaboration, K. Abe *et al.*, *Phys. Rev. Lett.* **87**, 091802 (2001); *Phys. Rev. D* **66**, 032007 (2002).
9. Belle Collaboration, K. Abe *et al.*, *Phys. Rev. D* **66**, 071102 (2002).
10. BaBar Collaboration, B. Aubert *et al.*, *Phys. Rev. Lett.* **87**, 091801 (2001); *Phys. Rev. D* **66**, 032003 (2002); *Phys. Rev. Lett.* **89**, 201802 (2002).
11. T.E. Browder and R. Faccini, Annual Review of Nuclear and Particle Physics, **53**, 353 (2003).
12. Belle Collaboration, K. Abe *et al.*, hep-ex/0308036, BELLE-CONF-0353, contributed to the XXI International Symposium on Lepton and Photon Interactions at High Energies, Aug.11-16, 2003, Fermilab, Illinois, U.S.A.
13. A. Hoecker, H. Lacker, S. Laplace and F. LiDiberder, hep-ph/0104062.
14. O. Long, M. Baak, R. N. Cahn and D. Kirkby, hep-ex/0303030 to appear in *Phys. Rev. D*.
15. BaBar Collaboration, B. Aubert *et al.*, hep-ex/0303018, to appear in *Phys. Rev. Lett.*.
16. Belle Collaboration, K. Abe *et al.*, hep-ex/0308053, BELLE-CONF-0342.
17. BaBar Collaboration, B. Aubert *et al.*, hep-ex/0306052, to appear in *Phys. Rev. Lett.*.
18. BaBar Collaboration, B. Aubert *et al.*, hep-ex/0303004, *Phys. Rev. Lett.* **90**, 221801 (2003).
19. H. Jawahery, contributions to these proceedings.
20. BaBar Collaboration, B. Aubert *et al.*, BABAR-PLOT-0053; BABAR-PLOT-0056.
21. The selection requirements for $B \rightarrow \eta' K_S^0$ are discussed in Belle Collaboration, K.-F. Chen and K. Hara *et al.*, *Phys. Lett. B* **546**, 196 (2002).
22. Belle Collaboration, A. Garmash *et al.*, hep-ex/0307082 to appear in *Phys. Rev. D*.
23. Y. Grossman, Z. Ligeti, Y. Nir, and H. Quinn, hep-ph/0303171, *Phys. Rev. D* **68**, 015004 (2003).
24. Y. Grossman and M. P. Worah, *Phys. Lett. B* **395**, 241 (1997).
25. D. London and A. Soni, *Phys. Lett. B* **407**, 61 (1997); Y. Grossman, G. Isidori and M. P. Worah, *Phys. Rev. D* **58**, 057504 (1998).
26. Private communication, Livio Lancieri.
27. Belle Collaboration, K.-F. Chen and A. Bozek *et al.*, hep-ex/0307014.
28. Belle Collaboration, K. Abe *et al.*, hep-ex/0308035, to appear in *Phys. Rev. Lett.*.

DISCUSSION

Stefan Spanier (University of Tennessee):

- 1) Unfortunately, the plenary session gives the audience only a limited chance to help you to establish the results by asking detailed questions.
- 2) Knowing the previous value of $S = -0.7 \pm 0.6$ from Belle, the newly added statistics must lead to an unphysical value of $S < -1.4$ leading typically to large correlations in S and C (pathological behavior) in this new sample. How probable is the value in the new sample?
- 3) How strong is the CP -asymmetry in the background?

Tom Browder:

- 1) A special breakout session is planned later in the Symposium.
- 2) For a true value near $S = -1$, the values in the new sample are quite consistent with Toy Monte Carlo studies. There is no statistically pathological behaviour in either old or new data samples. The observed errors are actually slightly larger than expected.

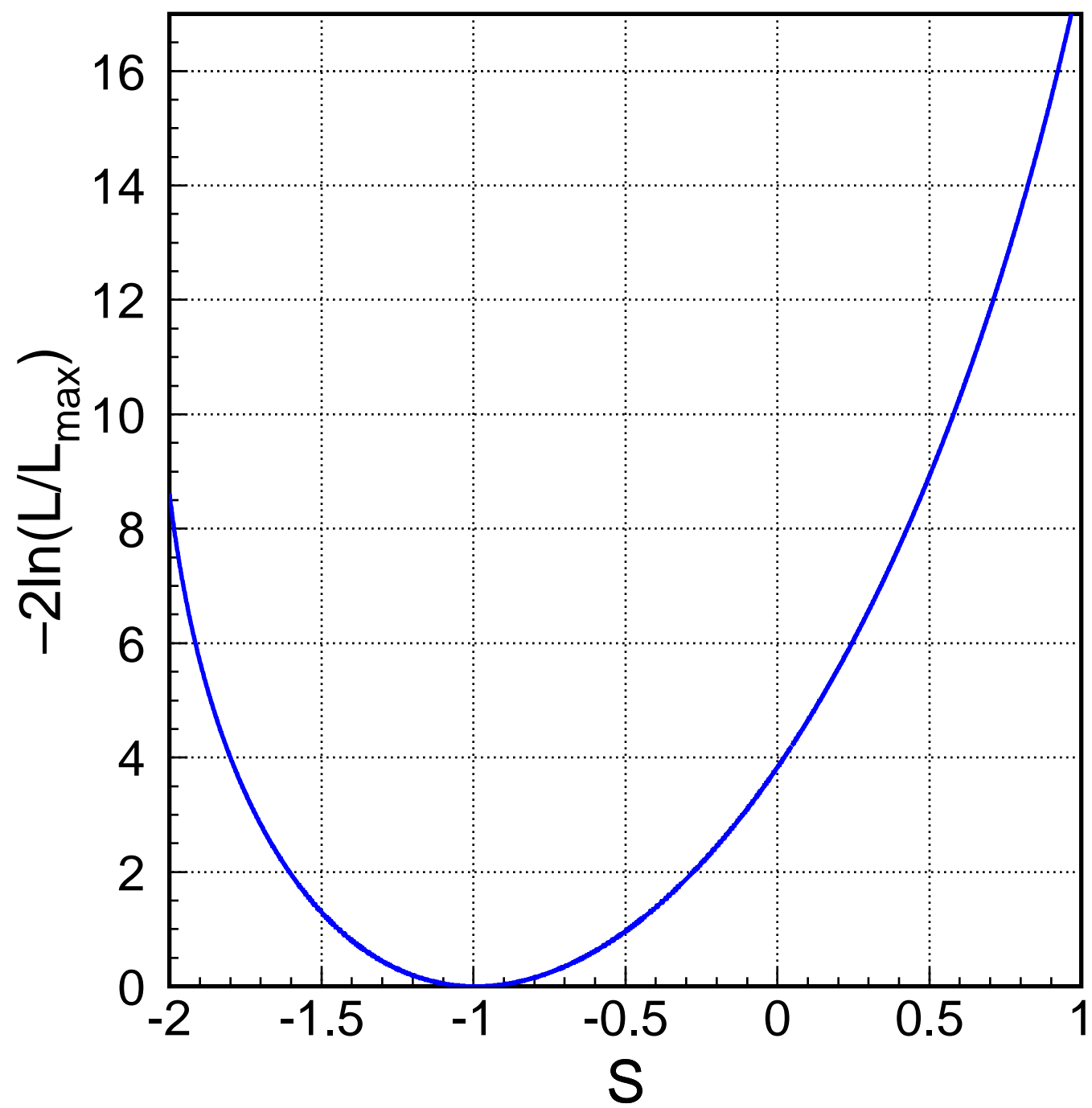
- 3) The background from $B \rightarrow f_0 K_S^0$ and $B \rightarrow K^+ K^- K_S^0$ decays is small and the CP -asymmetry from these backgrounds is included in the systematic error.

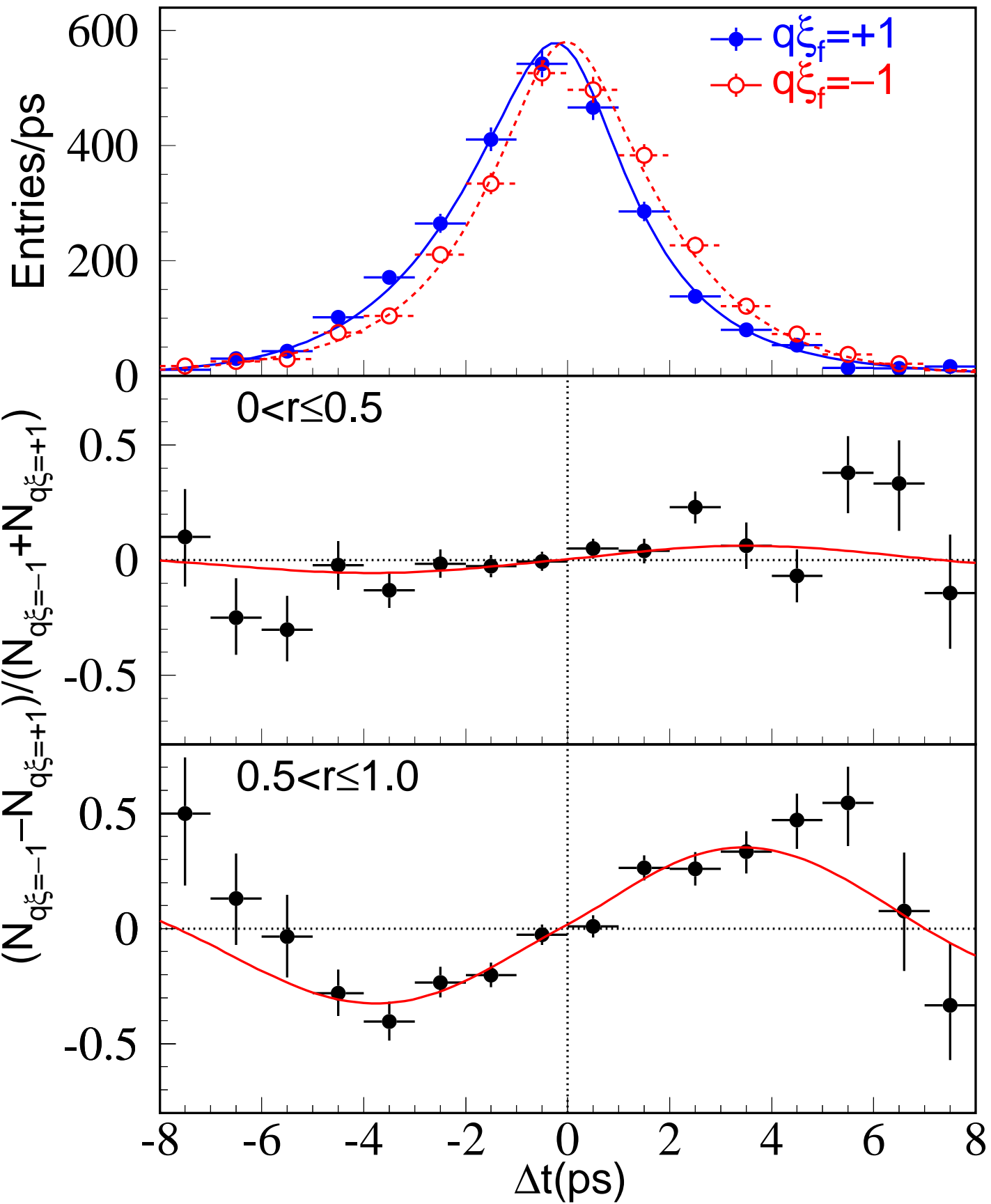
Alex Kagan (Cincinnati): Can you show the raw BaBar data for $S(\phi K_S^0)$ again?

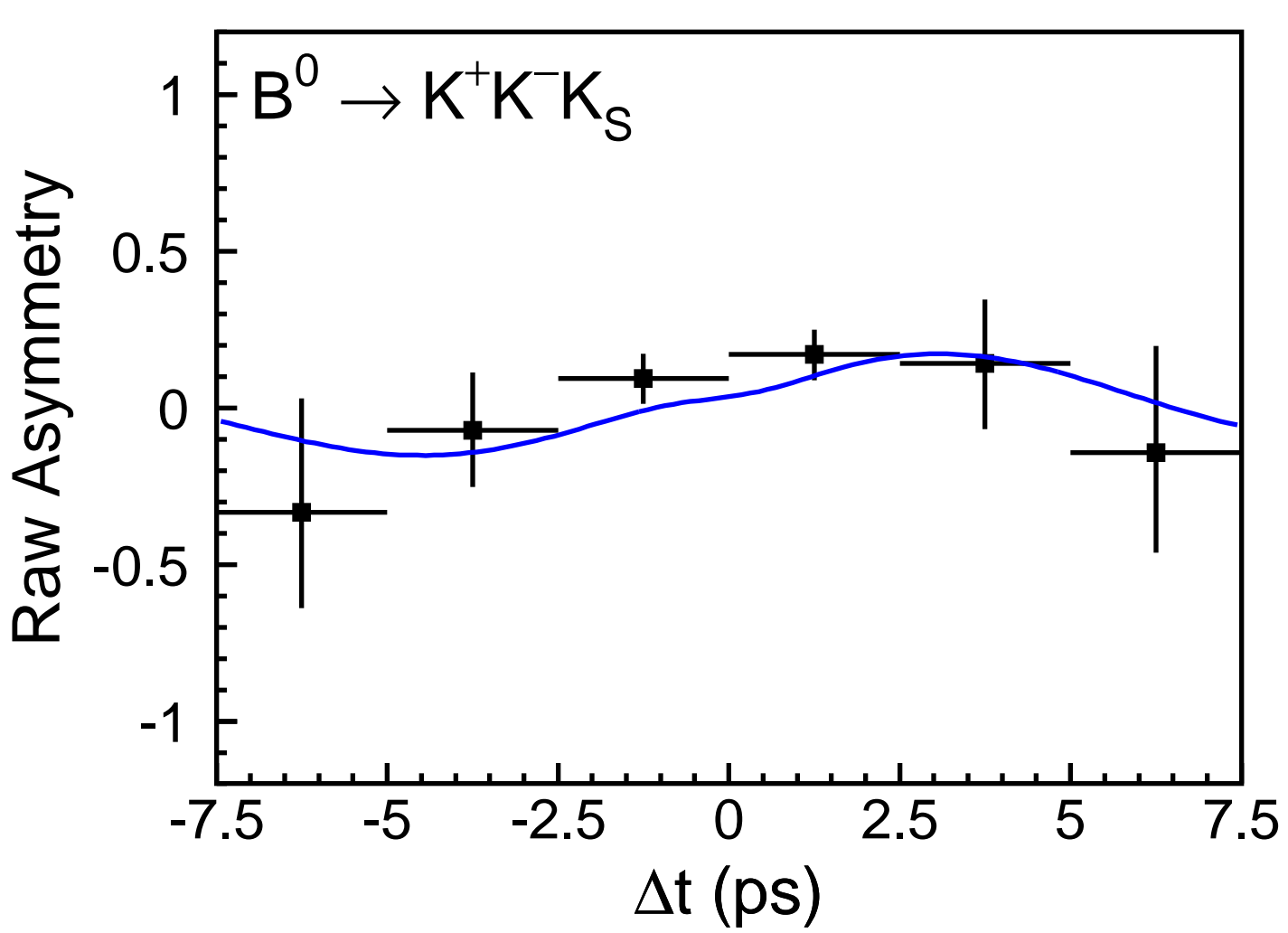
Tom Browder: Yes. Note that a figure with this data was included in the talk and appears in the Proceedings.

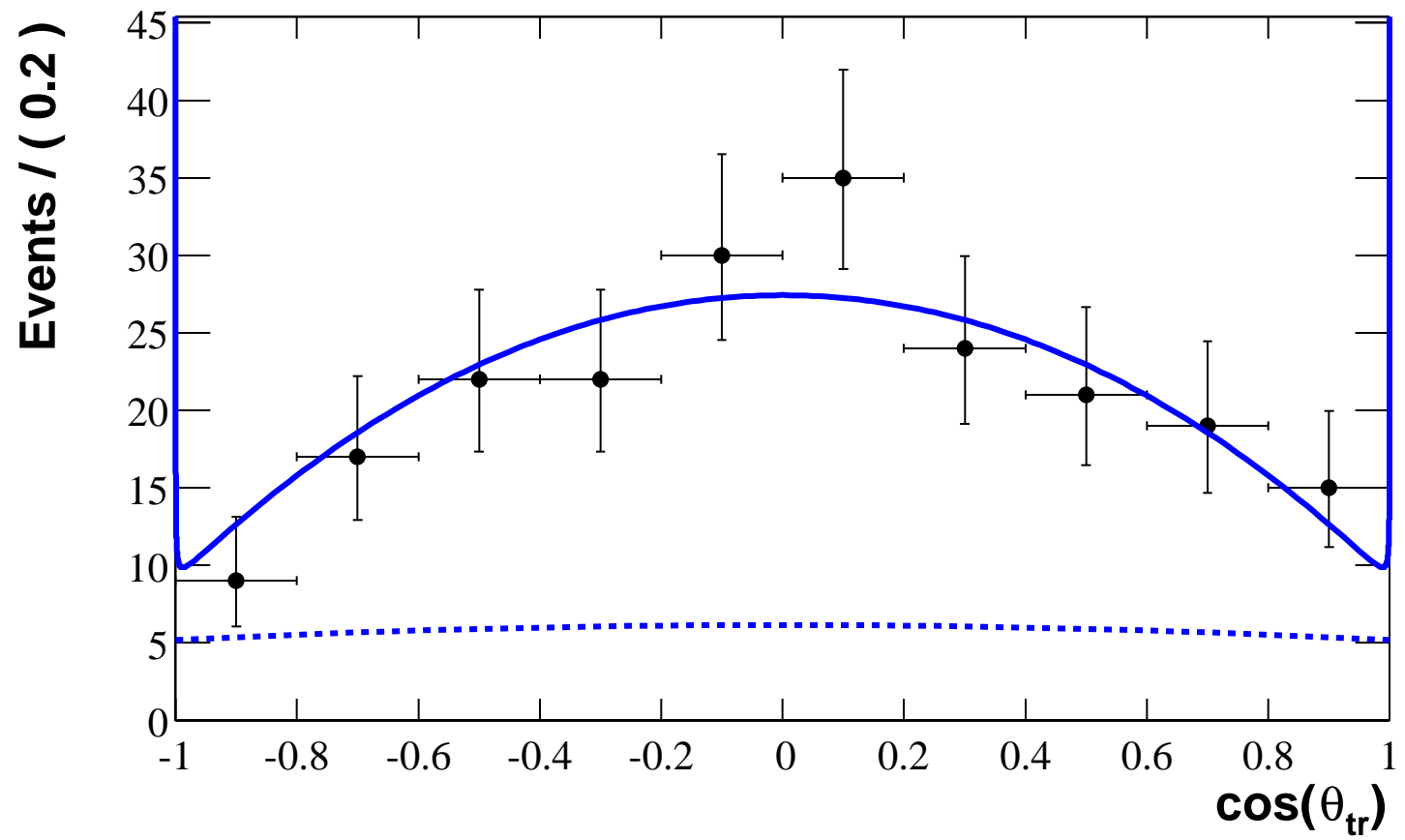
Hitoshi Murayama (Berkeley): On the ϕK_S^0 mode, the change in the BaBar result was attributed to a statistical fluctuation. They have added only 40% more data. How is that possible? Do you have a breakdown of the asymmetry between the previous and new data samples?

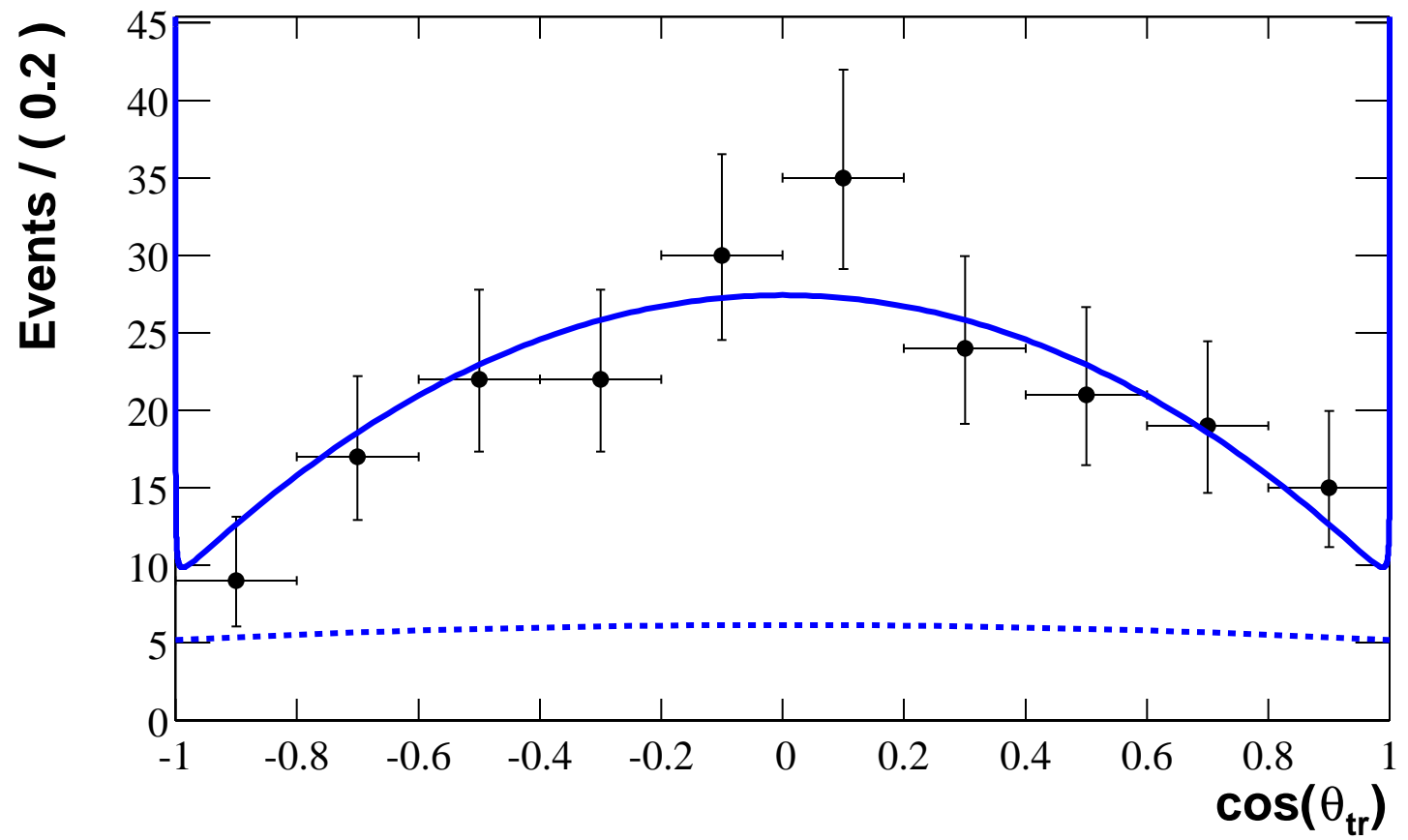
Tom Browder: Not only was more data added, but the old BaBar data sample was also reprocessed. After reprocessing, a small number of events changed from B^0 tags to \bar{B}^0 tags (or vice versa). This accounts for the shift in the central value.

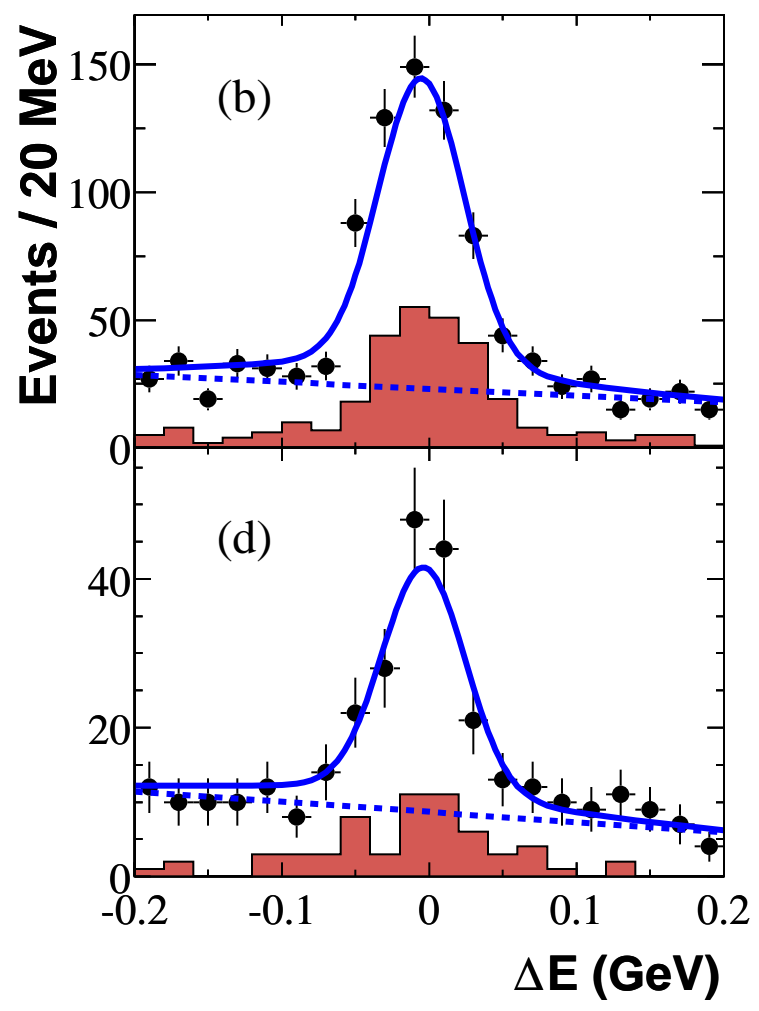
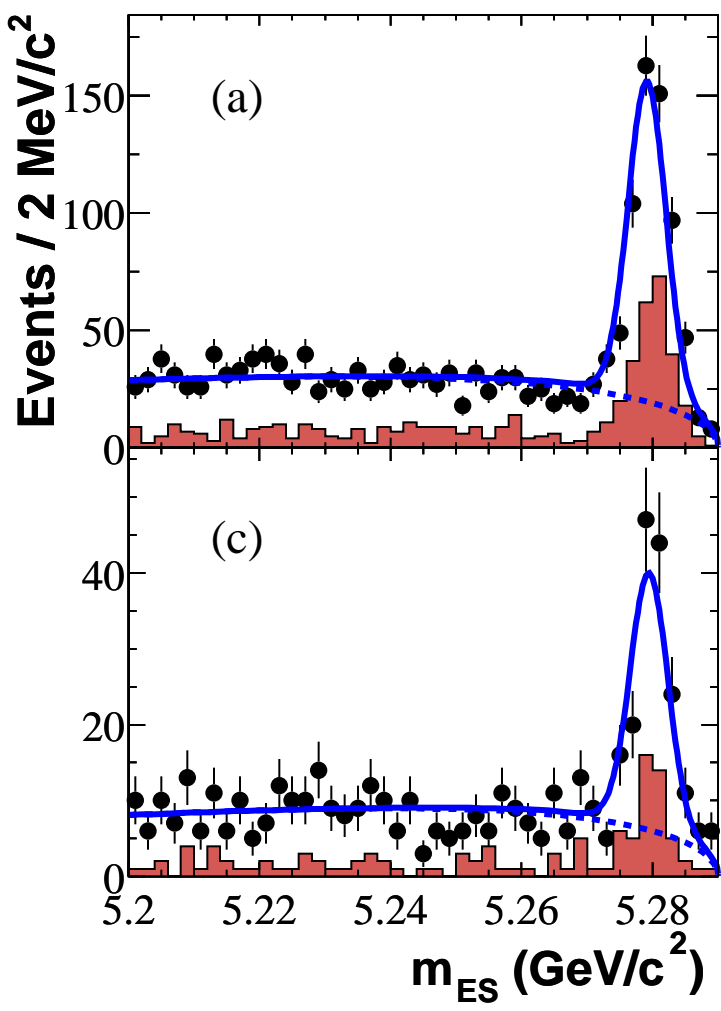






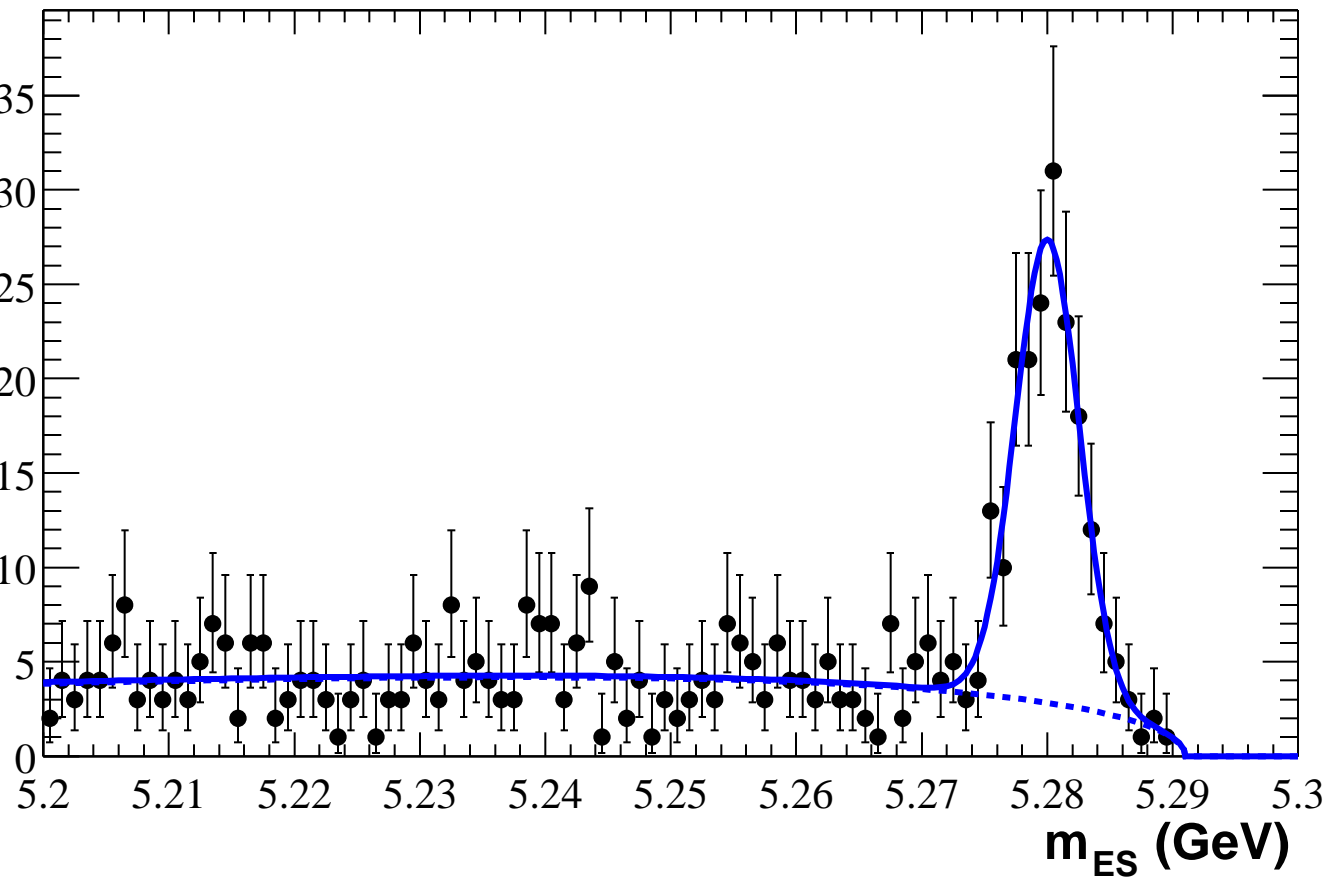






(c)

Events / (0.001 GeV)



Study of Time-Dependent CP Asymmetry in Neutral B Decays to $J/\psi \pi^0$

B. Aubert,¹ R. Barate,¹ D. Boutigny,¹ J.-M. Gaillard,¹ A. Hicheur,¹ Y. Karyotakis,¹ J. P. Lees,¹ P. Robbe,¹ V. Tisserand,¹ A. Zghiche,¹ A. Palano,² A. Pompili,² J. C. Chen,³ N. D. Qi,³ G. Rong,³ P. Wang,³ Y. S. Zhu,³ G. Eigen,⁴ I. Ofte,⁴ B. Stugu,⁴ G. S. Abrams,⁵ A. W. Borgland,⁵ A. B. Breon,⁵ D. N. Brown,⁵ J. Button-Shafer,⁵ R. N. Cahn,⁵ E. Charles,⁵ M. S. Gill,⁵ A. V. Gritsan,⁵ Y. Groysman,⁵ R. G. Jacobsen,⁵ R. W. Kadel,⁵ J. Kadyk,⁵ L. T. Kerth,⁵ Yu. G. Kolomensky,⁵ J. F. Kral,⁵ G. Kukartsev,⁵ C. LeClerc,⁵ M. E. Levi,⁵ G. Lynch,⁵ L. M. Mir,⁵ P. J. Oddone,⁵ T. J. Orimoto,⁵ M. Pripstein,⁵ N. A. Roe,⁵ A. Romosan,⁵ M. T. Ronan,⁵ V. G. Shelkov,⁵ A. V. Telnov,⁵ W. A. Wenzel,⁵ T. J. Harrison,⁶ C. M. Hawkes,⁶ D. J. Knowles,⁶ R. C. Penny,⁶ A. T. Watson,⁶ N. K. Watson,⁶ T. Deppermann,⁷ K. Goetzen,⁷ H. Koch,⁷ B. Lewandowski,⁷ M. Pelizaeus,⁷ K. Peters,⁷ H. Schmuecker,⁷ M. Steinke,⁷ N. R. Barlow,⁸ W. Bhimji,⁸ J. T. Boyd,⁸ N. Chevalier,⁸ P. J. Clark,⁸ W. N. Cottingham,⁸ C. Mackay,⁸ F. F. Wilson,⁸ C. Hearty,⁹ T. S. Mattison,⁹ J. A. McKenna,⁹ D. Thiessen,⁹ P. Kyberd,¹⁰ A. K. McKemey,¹⁰ V. E. Blinov,¹¹ A. D. Bukan,¹¹ V. B. Golubev,¹¹ V. N. Ivanchenko,¹¹ E. A. Kravchenko,¹¹ A. P. Onuchin,¹¹ S. I. Serednyakov,¹¹ Yu. I. Skovpen,¹¹ E. P. Solodov,¹¹ A. N. Yushkov,¹¹ D. Best,¹² M. Chao,¹² D. Kirkby,¹² A. J. Lankford,¹² M. Mandelkern,¹² S. McMahon,¹² R. K. Mommesen,¹² W. Roethel,¹² D. P. Stoker,¹² C. Buchanan,¹³ H. K. Hadavand,¹⁴ E. J. Hill,¹⁴ D. B. MacFarlane,¹⁴ H. P. Paar,¹⁴ Sh. Rahatlou,¹⁴ U. Schwanke,¹⁴ V. Sharma,¹⁴ J. W. Berryhill,¹⁵ C. Campagnari,¹⁵ B. Dahmes,¹⁵ N. Kuznetsova,¹⁵ S. L. Levy,¹⁵ O. Long,¹⁵ A. Lu,¹⁵ M. A. Mazur,¹⁵ J. D. Richman,¹⁵ W. Verkerke,¹⁵ J. Beringer,¹⁶ A. M. Eisner,¹⁶ C. A. Heusch,¹⁶ W. S. Lockman,¹⁶ T. Schalk,¹⁶ R. E. Schmitz,¹⁶ B. A. Schumm,¹⁶ A. Seiden,¹⁶ M. Turri,¹⁶ W. Walkowiak,¹⁶ D. C. Williams,¹⁶ M. G. Wilson,¹⁶ J. Albert,¹⁷ E. Chen,¹⁷ G. P. Dubois-Felsmann,¹⁷ A. Dvoretskii,¹⁷ D. G. Hitlin,¹⁷ I. Narsky,¹⁷ F. C. Porter,¹⁷ A. Ryd,¹⁷ A. Samuel,¹⁷ S. Yang,¹⁷ S. Jayatilleke,¹⁸ G. Mancinelli,¹⁸ B. T. Meadows,¹⁸ M. D. Sokoloff,¹⁸ T. Barillari,¹⁹ F. Blanc,¹⁹ P. Bloom,¹⁹ W. T. Ford,¹⁹ U. Nauenberg,¹⁹ A. Olivas,¹⁹ P. Rankin,¹⁹ J. Roy,¹⁹ J. G. Smith,¹⁹ W. C. van Hoek,¹⁹ L. Zhang,¹⁹ J. L. Harton,²⁰ T. Hu,²⁰ A. Soffer,²⁰ W. H. Toki,²⁰ R. J. Wilson,²⁰ J. Zhang,²⁰ D. Altenburg,²¹ T. Brandt,²¹ J. Brose,²¹ T. Colberg,²¹ M. Dickopp,²¹ R. S. Dubitzky,²¹ A. Hauke,²¹ H. M. Lacker,²¹ E. Maly,²¹ R. Müller-Pfefferkorn,²¹ R. Nogowski,²¹ S. Otto,²¹ K. R. Schubert,²¹ R. Schwierz,²¹ B. Spaan,²¹ L. Wilden,²¹ D. Bernard,²² G. R. Bonneau,²² F. Brochard,²² J. Cohen-Tanugi,²² S. T'Jampens,²² Ch. Thiebaut,²² G. Vasileiadis,²² M. Verderi,²² R. Bernet,²³ A. Khan,²³ D. Lavin,²³ F. Muheim,²³ S. Playfer,²³ J. E. Swain,²³ J. Tinslay,²³ C. Borean,²⁴ C. Bozzi,²⁴ L. Piemontese,²⁴ A. Sarti,²⁴ E. Treadwell,²⁵ F. Anulli,^{26,*} R. Baldini-Ferroli,²⁶ A. Calcaterra,²⁶ R. de Sangro,²⁶ D. Falciai,²⁶ G. Finocchiaro,²⁶ P. Patteri,²⁶ I. M. Peruzzi,^{26,*} M. Piccolo,²⁶ A. Zallo,²⁶ A. Buzzo,²⁷ R. Contri,²⁷ G. Crosetti,²⁷ M. Lo Vetere,²⁷ M. Macri,²⁷ M. R. Monge,²⁷ S. Passaggio,²⁷ F. C. Pastore,²⁷ C. Patrignani,²⁷ E. Robutti,²⁷ A. Santroni,²⁷ S. Tosi,²⁷ S. Bailey,²⁸ M. Morii,²⁸ G. J. Grenier,²⁹ S.-J. Lee,²⁹ U. Mallik,²⁹ J. Cochran,³⁰ H. B. Crawley,³⁰ J. Lamsa,³⁰ W. T. Meyer,³⁰ S. Prell,³⁰ E. I. Rosenberg,³⁰ J. Yi,³⁰ M. Davier,³¹ G. Grosdidier,³¹ A. Höcker,³¹ S. Laplace,³¹ F. Le Diberder,³¹ V. Lepeltier,³¹ A. M. Lutz,³¹ T. C. Petersen,³¹ S. Plaszczynski,³¹ M. H. Schune,³¹ L. Tantot,³¹ G. Wormser,³¹ R. M. Bionta,³² V. Brigljević,³² C. H. Cheng,³² D. J. Lange,³² D. M. Wright,³² A. J. Bevan,³³ J. R. Fry,³³ E. Gabathuler,³³ R. Gamet,³³ M. Kay,³³ D. J. Payne,³³ R. J. Sloane,³³ C. Touramanis,³³ M. L. Aspinwall,³⁴ D. A. Bowerman,³⁴ P. D. Dauncey,³⁴ U. Egede,³⁴ I. Eschrich,³⁴ G. W. Morton,³⁴ J. A. Nash,³⁴ P. Sanders,³⁴ G. P. Taylor,³⁴ J. J. Back,³⁵ G. Bellodi,³⁵ P. F. Harrison,³⁵ H. W. Shorthouse,³⁵ P. Strother,³⁵ P. B. Vidal,³⁵ G. Cowan,³⁶ H. U. Flaecher,³⁶ S. George,³⁶ M. G. Green,³⁶ A. Kurup,³⁶ C. E. Marker,³⁶ T. R. McMahon,³⁶ S. Ricciardi,³⁶ F. Salvatore,³⁶ G. Vaitsas,³⁶ M. A. Winter,³⁶ D. Brown,³⁷ C. L. Davis,³⁷ J. Allison,³⁸ R. J. Barlow,³⁸ A. C. Forti,³⁸ P. A. Hart,³⁸ F. Jackson,³⁸ G. D. Lafferty,³⁸ A. J. Lyon,³⁸ J. H. Weatherall,³⁸ J. C. Williams,³⁸ A. Farbin,³⁹ A. Jawahery,³⁹ D. Kovalskyi,³⁹ C. K. Lae,³⁹ V. Lillard,³⁹ D. A. Roberts,³⁹ G. Blaylock,⁴⁰ C. Dallapiccola,⁴⁰ K. T. Flood,⁴⁰ S. S. Hertzbach,⁴⁰ R. Kofler,⁴⁰ V. B. Koptchev,⁴⁰ T. B. Moore,⁴⁰ H. Staengle,⁴⁰ S. Willocq,⁴⁰ R. Cowan,⁴¹ G. Sciolla,⁴¹ F. Taylor,⁴¹ R. K. Yamamoto,⁴¹ D. J. J. Mangeol,⁴² M. Milek,⁴² P. M. Patel,⁴² F. Palombo,⁴³ J. M. Bauer,⁴⁴ L. Cremaldi,⁴⁴ V. Eschenburg,⁴⁴ R. Kroeger,⁴⁴ J. Reidy,⁴⁴ D. A. Sanders,⁴⁴ D. J. Summers,⁴⁴ H. W. Zhao,⁴⁴ C. Hast,⁴⁵ P. Taras,⁴⁵ H. Nicholson,⁴⁶ C. Cartaro,⁴⁷ N. Cavallo,⁴⁷ G. De Nardo,⁴⁷ F. Fabozzi,^{47,†} C. Gatto,⁴⁷ L. Lista,⁴⁷ P. Paolucci,⁴⁷ D. Piccolo,⁴⁷ C. Sciacca,⁴⁷ M. A. Baak,⁴⁸ G. Raven,⁴⁸

J. M. LoSecco,⁴⁹ T. A. Gabriel,⁵⁰ B. Brau,⁵¹ T. Pulliam,⁵¹ J. Brau,⁵² R. Frey,⁵² M. Iwasaki,⁵² C. T. Potter,⁵² N. B. Sinev,⁵² D. Strom,⁵² E. Torrence,⁵² F. Colecchia,⁵³ A. Dorigo,⁵³ F. Galeazzi,⁵³ M. Margoni,⁵³ M. Morandin,⁵³ M. Posocco,⁵³ M. Rotondo,⁵³ F. Simonetto,⁵³ R. Stroili,⁵³ G. Tiozzo,⁵³ C. Voci,⁵³ M. Benayoun,⁵⁴ H. Briand,⁵⁴ J. Chauveau,⁵⁴ P. David,⁵⁴ Ch. de la Vaissière,⁵⁴ L. Del Buono,⁵⁴ O. Hamon,⁵⁴ Ph. Leruste,⁵⁴ J. Ocariz,⁵⁴ M. Pivk,⁵⁴ L. Roos,⁵⁴ J. Stark,⁵⁴ P. F. Manfredi,⁵⁵ V. Re,⁵⁵ L. Gladney,⁵⁶ Q. H. Guo,⁵⁶ J. Panetta,⁵⁶ C. Angelini,⁵⁷ G. Batignani,⁵⁷ S. Bettarini,⁵⁷ M. Bondioli,⁵⁷ F. Bucci,⁵⁷ G. Calderini,⁵⁷ M. Carpinelli,⁵⁷ F. Forti,⁵⁷ M. A. Giorgi,⁵⁷ A. Lusiani,⁵⁷ G. Marchiori,⁵⁷ F. Martinez-Vidal,⁵⁷ M. Morganti,⁵⁷ N. Neri,⁵⁷ E. Paoloni,⁵⁷ M. Rama,⁵⁷ G. Rizzo,⁵⁷ F. Sandrelli,⁵⁷ G. Triggiani,⁵⁷ J. Walsh,⁵⁷ M. Haire,⁵⁸ D. Judd,⁵⁸ K. Paick,⁵⁸ D. E. Wagoner,⁵⁸ N. Danielson,⁵⁹ P. Elmer,⁵⁹ C. Lu,⁵⁹ V. Miftakov,⁵⁹ J. Olsen,⁵⁹ A. J. S. Smith,⁵⁹ E. W. Varnes,⁵⁹ F. Bellini,⁶⁰ G. Cavoto,^{59,60} D. del Re,⁶⁰ R. Faccini,^{14,60} F. Ferrarotto,⁶⁰ F. Ferroni,⁶⁰ M. Gaspero,⁶⁰ E. Leonardi,⁶⁰ M. A. Mazzoni,⁶⁰ S. Morganti,⁶⁰ M. Pierini,⁶⁰ G. Piredda,⁶⁰ F. Safai Tehrani,⁶⁰ M. Serra,⁶⁰ C. Voena,⁶⁰ S. Christ,⁶¹ G. Wagner,⁶¹ R. Waldi,⁶¹ T. Adye,⁶² N. De Groot,⁶² B. Franek,⁶² N. I. Geddes,⁶² G. P. Gopal,⁶² E. O. Olaiya,⁶² S. M. Xella,⁶² R. Aleksan,⁶³ S. Emery,⁶³ A. Gaidot,⁶³ S. F. Ganzhur,⁶³ P.-F. Giraud,⁶³ G. Hamel de Monchenault,⁶³ W. Kozanecki,⁶³ M. Langer,⁶³ G. W. London,⁶³ B. Mayer,⁶³ G. Schott,⁶³ G. Vasseur,⁶³ Ch. Yeche,⁶³ M. Zito,⁶³ M. V. Purohit,⁶⁴ A. W. Weidemann,⁶⁴ F. X. Yumiceva,⁶⁴ D. Aston,⁶⁵ R. Bartoldus,⁶⁵ N. Berger,⁶⁵ A. M. Boyarski,⁶⁵ O. L. Buchmueller,⁶⁵ M. R. Convery,⁶⁵ D. P. Coupal,⁶⁵ D. Dong,⁶⁵ J. Dorfan,⁶⁵ W. Dunwoodie,⁶⁵ R. C. Field,⁶⁵ T. Glanzman,⁶⁵ S. J. Gowdy,⁶⁵ E. Grauges-Pous,⁶⁵ T. Hadig,⁶⁵ V. Halyo,⁶⁵ T. Hrynowa,⁶⁵ W. R. Innes,⁶⁵ C. P. Jessop,⁶⁵ M. H. Kelsey,⁶⁵ P. Kim,⁶⁵ M. L. Kocian,⁶⁵ U. Langenegger,⁶⁵ D. W. G. S. Leith,⁶⁵ S. Luitz,⁶⁵ V. Luth,⁶⁵ H. L. Lynch,⁶⁵ H. Marsiske,⁶⁵ S. Menke,⁶⁵ R. Messner,⁶⁵ D. R. Muller,⁶⁵ C. P. O'Grady,⁶⁵ V. E. Ozcan,⁶⁵ A. Perazzo,⁶⁵ M. Perl,⁶⁵ S. Petrak,⁶⁵ B. N. Ratcliff,⁶⁵ S. H. Robertson,⁶⁵ A. A. Roodman,⁶⁵ A. A. Salnikov,⁶⁵ T. Schietinger,⁶⁵ R. H. Schindler,⁶⁵ J. Schwiening,⁶⁵ G. Simi,⁶⁵ A. Snyder,⁶⁵ A. Soha,⁶⁵ J. Stelzer,⁶⁵ D. Su,⁶⁵ M. K. Sullivan,⁶⁵ H. A. Tanaka,⁶⁵ J. Va'vra,⁶⁵ S. R. Wagner,⁶⁵ M. Weaver,⁶⁵ A. J. R. Weinstein,⁶⁵ W. J. Wisniewski,⁶⁵ D. H. Wright,⁶⁵ C. C. Young,⁶⁵ P. R. Burchat,⁶⁶ T. I. Meyer,⁶⁶ C. Roat,⁶⁶ S. Ahmed,⁶⁷ W. Bugg,⁶⁸ M. Krishnamurthy,⁶⁸ S. M. Spanier,⁶⁸ R. Eckmann,⁶⁹ H. Kim,⁶⁹ J. L. Ritchie,⁶⁹ R. F. Schwitters,⁶⁹ J. M. Izen,⁷⁰ I. Kitayama,⁷⁰ X. C. Lou,⁷⁰ F. Bianchi,⁷¹ M. Bona,⁷¹ D. Gamba,⁷¹ L. Bosisio,⁷² G. Della Ricca,⁷² S. Dittongo,⁷² S. Grancagnolo,⁷² L. Lanceri,⁷² P. Poropat,⁷² L. Vitale,⁷² G. Vuagnin,⁷² R. S. Panvini,⁷³ S. Banerjee,⁷⁴ C. M. Brown,⁷⁴ D. Fortin,⁷⁴ P. D. Jackson,⁷⁴ R. Kowalewski,⁷⁴ J. M. Roney,⁷⁴ H. R. Band,⁷⁵ S. Dasu,⁷⁵ M. Datta,⁷⁵ A. M. Eichenbaum,⁷⁵ H. Hu,⁷⁵ J. R. Johnson,⁷⁵ R. Liu,⁷⁵ F. Di Lodovico,⁷⁵ A. K. Mohapatra,⁷⁵ Y. Pan,⁷⁵ R. Prepost,⁷⁵ S. J. Sekula,⁷⁵ J. H. von Wimmersperg-Toeller,⁷⁵ J. Wu,⁷⁵ S. L. Wu,⁷⁵ Z. Yu,⁷⁵ and H. Neal⁷⁶

(The BABAR Collaboration)

¹*Laboratoire de Physique des Particules, F-74941 Annecy-le-Vieux, France*

²*Università di Bari, Dipartimento di Fisica and INFN, I-70126 Bari, Italy*

³*Institute of High Energy Physics, Beijing 100039, China*

⁴*University of Bergen, Inst. of Physics, N-5007 Bergen, Norway*

⁵*Lawrence Berkeley National Laboratory and University of California, Berkeley, CA 94720, USA*

⁶*University of Birmingham, Birmingham, B15 2TT, United Kingdom*

⁷*Ruhr Universität Bochum, Institut für Experimentalphysik 1, D-44780 Bochum, Germany*

⁸*University of Bristol, Bristol BS8 1TL, United Kingdom*

⁹*University of British Columbia, Vancouver, BC, Canada V6T 1Z1*

¹⁰*Brunel University, Uxbridge, Middlesex UB8 3PH, United Kingdom*

¹¹*Budker Institute of Nuclear Physics, Novosibirsk 630090, Russia*

¹²*University of California at Irvine, Irvine, CA 92697, USA*

¹³*University of California at Los Angeles, Los Angeles, CA 90024, USA*

¹⁴*University of California at San Diego, La Jolla, CA 92093, USA*

¹⁵*University of California at Santa Barbara, Santa Barbara, CA 93106, USA*

¹⁶*University of California at Santa Cruz, Institute for Particle Physics, Santa Cruz, CA 95064, USA*

¹⁷*California Institute of Technology, Pasadena, CA 91125, USA*

¹⁸*University of Cincinnati, Cincinnati, OH 45221, USA*

¹⁹*University of Colorado, Boulder, CO 80309, USA*

²⁰*Colorado State University, Fort Collins, CO 80523, USA*

²¹*Technische Universität Dresden, Institut für Kern- und Teilchenphysik, D-01062 Dresden, Germany*

²²*Ecole Polytechnique, LLR, F-91128 Palaiseau, France*

²³*University of Edinburgh, Edinburgh EH9 3JZ, United Kingdom*

²⁴*Università di Ferrara, Dipartimento di Fisica and INFN, I-44100 Ferrara, Italy*

²⁵*Florida A&M University, Tallahassee, FL 32307, USA*

²⁶*Laboratori Nazionali di Frascati dell'INFN, I-00044 Frascati, Italy*
²⁷*Università di Genova, Dipartimento di Fisica and INFN, I-16146 Genova, Italy*
²⁸*Harvard University, Cambridge, MA 02138, USA*
²⁹*University of Iowa, Iowa City, IA 52242, USA*
³⁰*Iowa State University, Ames, IA 50011-3160, USA*
³¹*Laboratoire de l'Accélérateur Linéaire, F-91898 Orsay, France*
³²*Lawrence Livermore National Laboratory, Livermore, CA 94550, USA*
³³*University of Liverpool, Liverpool L69 3BX, United Kingdom*
³⁴*University of London, Imperial College, London, SW7 2BW, United Kingdom*
³⁵*Queen Mary, University of London, E1 4NS, United Kingdom*
³⁶*University of London, Royal Holloway and Bedford New College, Egham, Surrey TW20 0EX, United Kingdom*
³⁷*University of Louisville, Louisville, KY 40292, USA*
³⁸*University of Manchester, Manchester M13 9PL, United Kingdom*
³⁹*University of Maryland, College Park, MD 20742, USA*
⁴⁰*University of Massachusetts, Amherst, MA 01003, USA*
⁴¹*Massachusetts Institute of Technology, Laboratory for Nuclear Science, Cambridge, MA 02139, USA*
⁴²*McGill University, Montréal, QC, Canada H3A 2T8*
⁴³*Università di Milano, Dipartimento di Fisica and INFN, I-20133 Milano, Italy*
⁴⁴*University of Mississippi, University, MS 38677, USA*
⁴⁵*Université de Montréal, Laboratoire René J. A. Lévesque, Montréal, QC, Canada H3C 3J7*
⁴⁶*Mount Holyoke College, South Hadley, MA 01075, USA*
⁴⁷*Università di Napoli Federico II, Dipartimento di Scienze Fisiche and INFN, I-80126, Napoli, Italy*
⁴⁸*NIKHEF, National Institute for Nuclear Physics and High Energy Physics, 1009 DB Amsterdam, The Netherlands*
⁴⁹*University of Notre Dame, Notre Dame, IN 46556, USA*
⁵⁰*Oak Ridge National Laboratory, Oak Ridge, TN 37831, USA*
⁵¹*Ohio State University, Columbus, OH 43210, USA*
⁵²*University of Oregon, Eugene, OR 97403, USA*
⁵³*Università di Padova, Dipartimento di Fisica and INFN, I-35131 Padova, Italy*
⁵⁴*Universités Paris VI et VII, Lab de Physique Nucléaire H. E., F-75252 Paris, France*
⁵⁵*Università di Pavia, Dipartimento di Elettronica and INFN, I-27100 Pavia, Italy*
⁵⁶*University of Pennsylvania, Philadelphia, PA 19104, USA*
⁵⁷*Università di Pisa, Dipartimento di fisica, Scuola Normale Superiore and INFN, I-56010 Pisa, Italy*
⁵⁸*Prairie View A&M University, Prairie View, TX 77446, USA*
⁵⁹*Princeton University, Princeton, NJ 08544, USA*
⁶⁰*Università di Roma La Sapienza, Dipartimento di Fisica and INFN, I-00185 Roma, Italy*
⁶¹*Universität Rostock, D-18051 Rostock, Germany*
⁶²*Rutherford Appleton Laboratory, Chilton, Didcot, Oxon, OX11 0QX, United Kingdom*
⁶³*DAPNIA, Commissariat à l'Energie Atomique/Saclay, F-91191 Gif-sur-Yvette, France*
⁶⁴*University of South Carolina, Columbia, SC 29208, USA*
⁶⁵*Stanford Linear Accelerator Center, Stanford, CA 94309, USA*
⁶⁶*Stanford University, Stanford, CA 94305-4060, USA*
⁶⁷*State Univ. of New York, Albany, NY 12222, USA*
⁶⁸*University of Tennessee, Knoxville, TN 37996, USA*
⁶⁹*University of Texas at Austin, Austin, TX 78712, USA*
⁷⁰*University of Texas at Dallas, Richardson, TX 75083, USA*
⁷¹*Università di Torino, Dipartimento di Fisica Sperimentale and INFN, I-10125 Torino, Italy*
⁷²*Università di Trieste, Dipartimento di Fisica and INFN, I-34127 Trieste, Italy*
⁷³*Vanderbilt University, Nashville, TN 37235, USA*
⁷⁴*University of Victoria, Victoria, BC, Canada V8W 3P6*
⁷⁵*University of Wisconsin, Madison, WI 53706, USA*
⁷⁶*Yale University, New Haven, CT 06511, USA*

(Dated: March 14, 2003)

We present the first study of the time-dependent CP -violating asymmetry in $B^0 \rightarrow J/\psi \pi^0$ decays using e^+e^- annihilation data collected with the *BABAR* detector at the $\Upsilon(4S)$ resonance during the years 1999–2002 at the PEP-II asymmetric-energy B Factory at SLAC. Using approximately 88 million $B\bar{B}$ pairs, our results for the coefficients of the cosine and sine terms of the CP asymmetry are $C_{J/\psi \pi^0} = 0.38 \pm 0.41$ (stat) ± 0.09 (syst) and $S_{J/\psi \pi^0} = 0.05 \pm 0.49$ (stat) ± 0.16 (syst).

PACS numbers: 13.25.Hw, 12.15.Hh, 11.30.Er

The Standard Model of electroweak interactions describes CP violation in B -meson decays by a com-

plex phase in the three-generation Cabibbo-Kobayashi-Maskawa (CKM) quark-mixing matrix [1]. The $b \rightarrow c\bar{c}s$

modes such as $B^0 \rightarrow J/\psi K_s^0$ yield precise measurements of the quantity $\sin 2\beta$, where $\beta \equiv \arg[-V_{cd} V_{cb}^* / V_{td} V_{tb}^*]$ (see for example Refs. [2–4]). The decay $B^0 \rightarrow J/\psi \pi^0$ is a Cabibbo-suppressed $b \rightarrow c\bar{c}d$ transition. In the Standard Model both $B^0 \rightarrow J/\psi K_s^0$ and $B^0 \rightarrow J/\psi \pi^0$ have penguin amplitudes with the same weak phase as the tree amplitude, and an additional penguin amplitude with a different phase. In $B^0 \rightarrow J/\psi K_s^0$, the penguin amplitude with a different weak phase is suppressed by λ_{CKM}^2 , where λ_{CKM} is the sine of the Cabibbo angle, while in $B^0 \rightarrow J/\psi \pi^0$, the tree and each penguin amplitude are equal to leading order in λ_{CKM} . Therefore, $B^0 \rightarrow J/\psi \pi^0$ may have a CP asymmetry that differs from that of $B^0 \rightarrow J/\psi K_s^0$, with the size of the asymmetry serving as a probe of the penguin decay amplitudes in both modes.

BABAR has previously measured the $B^0 \rightarrow J/\psi \pi^0$ branching fraction, $(2.0 \pm 0.6 \text{ (stat)} \pm 0.2 \text{ (syst)}) \times 10^{-5}$ [5], using $\Upsilon(4S) \rightarrow B\bar{B}$ decays. For the CP asymmetry measurement, the flavor (B^0 or \bar{B}^0) of the B meson that decays to $J/\psi \pi^0$ is inferred, or tagged, using properties of the other B meson and the time evolution of the $B\bar{B}$ system. The decay time distributions, $f_+(\mathbf{f}_-)$, of B decays to a CP eigenstate with a B^0 (\bar{B}^0) flavor tag, are given by

$$f_{\pm}(\Delta t) = \frac{e^{-|\Delta t|/\tau_{B^0}}}{4\tau_{B^0}} \left[1 \pm S_{J/\psi\pi^0} \sin(\Delta m_d \Delta t) \mp C_{J/\psi\pi^0} \cos(\Delta m_d \Delta t) \right], \quad (1)$$

where $\Delta t = t_{\text{rec}} - t_{\text{tag}}$ is the difference between the proper decay time of the reconstructed B meson and the proper decay time of the tagging B meson, τ_{B^0} is the B^0 lifetime, and Δm_d is the B^0 - \bar{B}^0 oscillation frequency. The coefficients can be expressed in terms of a complex parameter λ , which depends on both the B^0 - \bar{B}^0 oscillation amplitude and the B^0 and \bar{B}^0 decay amplitudes to this final state [6]: $S_{J/\psi\pi^0} = 2\text{Im}\lambda/(1+|\lambda|^2)$ and $C_{J/\psi\pi^0} = (1-|\lambda|^2)/(1+|\lambda|^2)$. A decay amplitude with only a tree component would give $S_{J/\psi\pi^0} = -\sin 2\beta$ and $C_{J/\psi\pi^0} = 0$.

The data used in this measurement were collected with the *BABAR* detector [7] at the PEP-II storage ring in the years 1999 to 2002. Approximately 81 fb^{-1} of e^+e^- annihilation data recorded at the $\Upsilon(4S)$ resonance are used, corresponding to a sample of approximately 88 million $B\bar{B}$ pairs. An additional 5 fb^{-1} of data collected approximately 40 MeV below the $\Upsilon(4S)$ resonance are used to characterize non- $B\bar{B}$ background sources.

$B^0 \rightarrow J/\psi \pi^0$ candidates are selected (details are given in Ref. [5]) by identifying $J/\psi \rightarrow e^+e^-$ or $J/\psi \rightarrow \mu^+\mu^-$ decays and $\pi^0 \rightarrow \gamma\gamma$ decays. For the $J/\psi \rightarrow e^+e^-$ ($J/\psi \rightarrow \mu^+\mu^-$) channel, each lepton candidate must be consistent with the electron (muon) hypothesis. The invariant

TABLE I: Efficiencies for the requirement on the Fisher discriminant and flavor tagging, given independently, with statistical uncertainties.

Type of event	Efficiency (%)	
	Fisher	Tagging
$B^0 \rightarrow J/\psi \pi^0$	99.2 ± 0.1	65.6 ± 0.6
$B^0 \rightarrow J/\psi K_s^0(\pi^0\pi^0)$ bkg.	98.9 ± 0.1	65.6 ± 0.6
Inclusive J/ψ bkg.	94.9 ± 0.7	70.4 ± 1.4
$B\bar{B}$ generic bkg.	98.5 ± 0.4	61.1 ± 1.6
Continuum bkg.	28.6 ± 0.7	52.3 ± 0.8

mass of the lepton pair is required to be between 2.95 and $3.14 \text{ GeV}/c^2$, and 3.06 and $3.14 \text{ GeV}/c^2$, for the electron and muon channels, respectively. The photon candidates used to reconstruct the π^0 candidate are identified as clusters in the electromagnetic calorimeter (EMC) with polar angles between 0.410 and 2.409 rad, that are spatially separated from every charged track, and have a minimum energy of 30 MeV. The lateral energy distribution in the cluster is required to be consistent with that of a photon. The invariant mass of the photon pair is required to between 100 and $160 \text{ MeV}/c^2$. Finally, the J/ψ and π^0 candidates are assigned their nominal masses and combined using 4-momentum addition.

Two kinematic consistency requirements are applied to each B candidate. The difference, ΔE , between the B -candidate energy and the beam energy in the e^+e^- center-of-mass (CM) frame must be $-0.4 < \Delta E < 0.4 \text{ GeV}$. The beam-energy-substituted mass, $m_{\text{ES}} = \sqrt{(\sqrt{s}/2)^2 - (p_B^*)^2}$, must be greater than $5.2 \text{ GeV}/c^2$, where \sqrt{s} is the total CM energy and p_B^* is the B -candidate momentum in the CM frame.

A linear combination of several kinematic and topological variables, determined with a Fisher discriminant, provides additional separation between signal and $e^+e^- \rightarrow q\bar{q}$ ($q = u, d, s, c$) continuum background events. The Fisher discriminant uses the following inputs: the zeroth- and second-order Legendre polynomial momentum moments ($L_0 = \sum_i |\mathbf{p}_i^*|$ and $L_2 = \sum_i |\mathbf{p}_i^*| \frac{3\cos^2\theta_i - 1}{2}$, where \mathbf{p}_i^* are the CM momenta for the tracks and neutral calorimeter clusters that are not associated with the signal candidate, and θ_i are the angles between \mathbf{p}_i^* and the thrust axis of the signal candidate); the ratio of the second-order to zeroth-order Fox-Wolfram moments, again using just tracks and clusters not associated with the signal candidate; $|\cos\theta_T|$, where θ_T is the angle between the thrust axis of the B candidate and the thrust axis of the remaining tracks and clusters in the event; and $|\cos\theta_\ell|$, where θ_ℓ is defined as the angle between the negative lepton and B candidate directions in the J/ψ rest frame. The requirement placed on the Fisher discriminant is 99% efficient for signal and rejects 71% of the continuum background. The efficiencies for satisfying this requirement are summarized in Table I.

We split the backgrounds into four mutually exclusive categories, two of which have a J/ψ from B decays ($B \rightarrow J/\psi X$). The first background category is $B^0 \rightarrow J/\psi K_s^0(\pi^0\pi^0)$ decays where one of the π^0 mesons is nearly at rest in the e^+e^- CM frame. The second background category consists of other $B \rightarrow J/\psi X$ decays (inclusive J/ψ), which contribute through random combinations of J/ψ and π^0 candidates. The third and fourth categories consist of random combinations of particles in $B\bar{B}$ decays ($B\bar{B}$ generic) and continuum events, respectively. Monte Carlo simulation [8] is used to model aspects of the $B^0 \rightarrow J/\psi K_s^0(\pi^0\pi^0)$, inclusive J/ψ , and $B\bar{B}$ generic backgrounds. A sample (J/ψ_{fake}) selected from data taken below the $\Upsilon(4S)$ resonance is used to model the continuum background. In this case, the J/ψ candidate is reconstructed from two tracks that are not consistent with a lepton hypothesis. Monte Carlo simulation is used to check that this procedure, which increases the size of the sample, correctly models the continuum background.

The algorithm for B -flavor tagging assigns events to one of four hierarchical, mutually exclusive tagging categories, and is described in detail in Ref. [3]. The total tagging efficiency for the signal and each background source is given in Table I. Untagged events are excluded from further consideration. Vertex reconstruction and the determination of Δt follow the techniques detailed in Ref. [9]. We require $-20 < \Delta t < 20$ ps and an estimated uncertainty on Δt of less than 2.4 ps.

We extract the CP asymmetry by performing an unbinned extended maximum likelihood fit. The likelihood is constructed from the probability density functions (PDFs) for the variables m_{ES} , ΔE , and Δt . The quantity that is maximized is the logarithm of

$$\mathcal{L} = \frac{e^{-\sum_{j=1}^5 n_j}}{N!} \prod_{i=1}^N \sum_{j=1}^5 \left[f_j^{\alpha_i} n_j \prod_d \mathcal{P}_j^d \right], \quad (2)$$

where n_j is the number of events for each of the five hypotheses (one signal and four background) and N is the number of input events. The \mathcal{P}_j^d are the one- or two-dimensional PDFs for variables d , for each signal or background type. The parameters $f_j^{\alpha_i}$ are the tagging fractions for each of the tagging categories α_i (assigned for each event i) and each of the signal or background types j . For the $B^0 \rightarrow J/\psi \pi^0$ signal and $B^0 \rightarrow J/\psi K_s^0(\pi^0\pi^0)$ background, the values of $f_j^{\alpha_i}$ are measured with a sample (B_{flav}) of neutral B decays to flavor eigenstates consisting of the channels $D^{(*)-}h^+(h^+ = \pi^+, \rho^+, \text{ and } a_1^+)$ and $J/\psi K^{*0}(K^{*0} \rightarrow K^+\pi^-)$ [3]. Monte Carlo simulation is used to estimate the $f_j^{\alpha_i}$ values for the inclusive J/ψ and $B\bar{B}$ generic backgrounds, while the J/ψ_{fake} sample is used for the continuum background.

The signal m_{ES} distribution is modeled as the sum of two components. The first is a modified Gaussian function that, for values less than the mean, has a

width parameter that scales linearly with the distance from the mean. The second component, accounting for less than 6% of the distribution, is a threshold function [10], which is a phase-space distribution of the form $m_{\text{ES}} \sqrt{(1 - \frac{m_{\text{ES}}^2}{E_{\text{beam}}^2})} \exp(\xi(1 - \frac{m_{\text{ES}}^2}{E_{\text{beam}}^2}))$, with a kinematic cut-off at $E_{\text{beam}} = 5.289$ GeV and one free parameter ξ . The signal ΔE distribution is modeled by the sum of a Gaussian core with an asymmetric power-low tail [11] and a second order polynomial. The parameters of these PDFs are determined by fitting to a signal Monte Carlo sample. The peak position of the ΔE distribution is a free parameter of the full CP likelihood fit to allow for EMC energy scale uncertainties.

The kinematic variables m_{ES} and ΔE are correlated in the $B^0 \rightarrow J/\psi K_s^0(\pi^0\pi^0)$ and inclusive J/ψ backgrounds, so two-dimensional PDFs are employed for these modes. Variably-binned interpolated two-dimensional histograms of these variables are constructed from the relevant Monte Carlo samples.

The m_{ES} PDFs for the $B\bar{B}$ generic and continuum backgrounds are modeled by the threshold function given above, and the ΔE PDFs for these two backgrounds are modeled by second order polynomials. The parameters for these PDFs are obtained from the $B\bar{B}$ generic Monte Carlo sample and the J/ψ_{fake} sample.

The PDFs used to describe the Δt distributions of the signal and background sources are each a convolution of a resolution function \mathcal{R} and decay time distribution \mathcal{D} : $\mathcal{P}(\Delta t, \sigma_{\Delta t}) = \mathcal{R}(\delta t, \sigma_{\Delta t}) \otimes \mathcal{D}(\Delta t_{\text{true}})$, where Δt and Δt_{true} are the measured and true decay time differences, $\delta t = \Delta t - \Delta t_{\text{true}}$, and $\sigma_{\Delta t}$ is the estimated event-by-event error on Δt .

For the signal, the resolution function consists of the sum of three Gaussian distributions, the parameters of which are determined from the B_{flav} sample, as in the $B^0 \rightarrow J/\psi K_s^0$ measurement [9]. The decay time distribution is given by Eq. 1 modified for the effects of B -flavor tagging:

$$\mathcal{D}_{\alpha,f}^{\pm}(\Delta t) = \frac{e^{-|\Delta t|/\tau_{B^0}}}{4\tau_{B^0}} \{ (1 \mp \Delta w_{\alpha}) \pm S_f (1 - 2w_{\alpha}) \sin(\Delta m_d \Delta t) \mp C_f (1 - 2w_{\alpha}) \cos(\Delta m_d \Delta t) \}, \quad (3)$$

where $\mathcal{D}_{\alpha,f}^+(\mathcal{D}_{\alpha,f}^-)$ is for a $B^0(\bar{B}^0)$ tagging meson. The variable w_{α} is the average probability of incorrectly tagging a B^0 as a \bar{B}^0 ($w_{\alpha}^{B^0}$) or a \bar{B}^0 as a B^0 ($w_{\alpha}^{\bar{B}^0}$), and $\Delta w_{\alpha} = w_{\alpha}^{B^0} - w_{\alpha}^{\bar{B}^0}$. Both w_{α} and Δw_{α} are determined using the B_{flav} data sample [3]. We use the values $\Delta m_d = 0.489$ ps⁻¹ and $\tau_{B^0} = 1.542$ ps [12].

The PDF used to model the Δt distribution for the $B^0 \rightarrow J/\psi K_s^0(\pi^0\pi^0)$ background, which also includes a CP asymmetry, takes the same form as that for signal, but with $S_{J/\psi K_s^0} = \sin 2\beta = 0.74$ [3] and $C_{J/\psi K_s^0} = 0$.

The parameterizations of the Δt PDFs for the inclu-

TABLE II: Results of the CP likelihood fit, for the full region $-0.4 < \Delta E < 0.4$ GeV and $m_{ES} > 5.2$ GeV/c 2 . Errors are statistical only. The global correlation coefficient is 0.14 for $C_{J/\psi \pi^0}$ and 0.15 for $S_{J/\psi \pi^0}$.

	Fit results
$C_{J/\psi \pi^0}$	0.38 ± 0.41
$S_{J/\psi \pi^0}$	0.05 ± 0.49
Signal ΔE peak position (MeV)	-13.2 ± 7.2
$B^0 \rightarrow J/\psi \pi^0$ signal (events)	40 ± 7
$B^0 \rightarrow J/\psi K_s^0(\pi^0\pi^0)$ background (events)	140 ± 19
Inclusive J/ψ background (events)	109 ± 35
$B\bar{B}$ generic background (events)	52 ± 25
Continuum background (events)	97 ± 22

sive J/ψ and $B\bar{B}$ generic backgrounds each consist of prompt and exponential decay components. Decays appear to be prompt when particles from the reconstructed B are erroneously included in the tagging B vertex. For the $B\bar{B}$ generic background, the prompt and exponential components correspond to the cases where the two decay products forming the J/ψ come from both or just one of the B mesons, respectively. The fraction that is in the exponential component, the decay lifetime parameter, and the resolution parameters are determined from the Monte Carlo simulation.

The Δt PDF for the continuum background has only a prompt component and the resolution parameter values are obtained by fitting the J/ψ_{fake} sample.

The results of the CP asymmetry fit, for all free parameters, are shown in Table II. There are 40 ± 7 signal events in the total sample of 438 selected events. The projection in m_{ES} is shown in Fig. 1. The yields and asymmetry as functions of Δt , overlaid with projections of the likelihood fit results, are shown in Fig. 2. Repeating the fit with the added constraint $C_{J/\psi \pi^0} = 0$ does not significantly change the result for $S_{J/\psi \pi^0}$.

The dominant contributions to the systematic errors in $C_{J/\psi \pi^0}$ and $S_{J/\psi \pi^0}$ are summarized in Table III. The first class of uncertainties are those obtained by variation of the parameters used in the m_{ES} , ΔE , and Δt PDFs, where the dominant sources are the uncertainties in the signal ΔE PDF parameters. A systematic error to account for a correlation between the tails of the signal m_{ES} and ΔE distributions is obtained by using a two-dimensional PDF. Another contribution stems from the impact of EMC energy scale uncertainties on the modeling of the $B^0 \rightarrow J/\psi K_s^0(\pi^0\pi^0)$ background. An additional systematic uncertainty comes from the choice of the binning of the two-dimensional PDFs for the $B^0 \rightarrow J/\psi K_s^0(\pi^0\pi^0)$ and inclusive J/ψ backgrounds.

In summary, an unbinned extended maximum likelihood fit yields 40 ± 7 signal events and the parameters of time-dependent CP asymmetry for the decay $B^0 \rightarrow J/\psi \pi^0$: $C_{J/\psi \pi^0} = 0.38 \pm 0.41$ (stat) ± 0.09 (syst) and $S_{J/\psi \pi^0} = 0.05 \pm 0.49$ (stat) ± 0.16 (syst). Within the

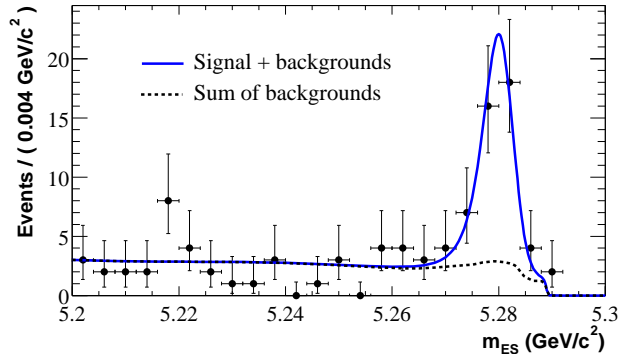


FIG. 1: Projection in m_{ES} for the results of the CP fit, displayed with the added requirement $-0.11 < \Delta E < 0.11$ GeV. In contrast, the CP fit uses the full ΔE region. In the further restricted region $m_{ES} > 5.27$ GeV/c 2 , there are 49 data events (points), of which about 12 events are fit as background. Here, $B^0 \rightarrow J/\psi K_s^0(\pi^0\pi^0)$ and inclusive J/ψ decays contribute to the enhancement in the background distribution at large m_{ES} .

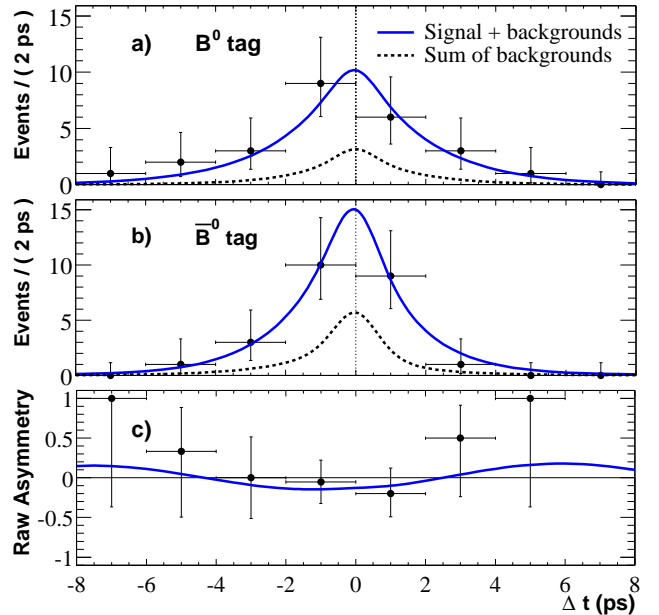


FIG. 2: Distributions of events a) with a B^0 tag (N_{B^0}), b) with a \bar{B}^0 tag ($N_{\bar{B}^0}$), and c) the raw asymmetry ($N_{B^0} - N_{\bar{B}^0}) / (N_{B^0} + N_{\bar{B}^0}$), as functions of Δt . Candidates in these plots are required to satisfy $-0.11 < \Delta E < 0.11$ GeV and $m_{ES} > 5.27$ GeV/c 2 . Of the 49 signal and background events in this region, 25 have a B^0 tag and 24 have a \bar{B}^0 tag, with fit background contributions of approximately 5 and 7 events, respectively. The curves are projections that use the values of the other variables in the likelihood to determine the contributions to the signal and backgrounds.

Standard Model formulation of CP asymmetries, these results demonstrate the possibility, with additional integrated luminosity, of observing penguin contributions in

TABLE III: Summary of systematic uncertainties.

Source	$C_{J/\psi \pi^0}$	$S_{J/\psi \pi^0}$
Parameter variations		
m_{ES} and ΔE parameters	0.05	0.13
Tagging fractions	0.00	0.01
Δt parameters	0.03	0.02
Additional systematics		
ΔE - m_{ES} correlation in signal	0.07	0.08
EMC energy scale $B^0 \rightarrow J/\psi K_S^0(\pi^0 \pi^0)$	0.01	0.00
Choice of two-D histogram PDFs	0.01	0.03
Beam spot, boost/vtx., misalignment	0.01	0.01
Total systematic uncertainty	0.09	0.16

$B^0 \rightarrow J/\psi \pi^0$. Such a measurement may experimentally constrain similar amplitudes in $B^0 \rightarrow J/\psi K_S^0$.

We are grateful for the excellent luminosity and machine conditions provided by our PEP-II colleagues, and for the substantial dedicated effort from the computing organizations that support *BABAR*. The collaborating institutions wish to thank SLAC for its support and kind hospitality. This work is supported by DOE and NSF (USA), NSERC (Canada), IHEP (China), CEA and CNRS-IN2P3 (France), BMBF and DFG (Germany), INFN (Italy), FOM (The Netherlands), NFR (Norway), MIST (Russia), and PPARC (United Kingdom). Individuals have received support from the A. P. Sloan Foundation, Research Corporation, and Alexander von Humboldt Foundation.

* Also with Università di Perugia, Perugia, Italy
 † Also with Università della Basilicata, Potenza, Italy
 ‡ Also with IFIC, Instituto de Física Corpuscular, CSIC-Universidad de Valencia, Valencia, Spain
 § Deceased

[1] N. Cabibbo, Phys. Rev. Lett. **10**, 531 (1963);
 M. Kobayashi and T. Maskawa, Prog. Th. Phys. **49**, 652 (1973).
 [2] *BABAR* Collaboration, B. Aubert *et al.*, Phys. Rev. Lett. **87**, 091801 (2001).
 [3] *BABAR* Collaboration, B. Aubert *et al.*, Phys. Rev. Lett. **89**, 201802 (2002).
 [4] *Belle* Collaboration, K. Abe *et al.*, Phys. Rev. Lett. **87**, 091802 (2001); Phys. Rev. D **66**, 071102 (2002).
 [5] *BABAR* Collaboration, B. Aubert *et al.*, Phys. Rev. D **65**, 032001 (2002).
 [6] See, for example, L. Wolfenstein, Phys. Rev. D **66**, 010001 (2002).
 [7] *BABAR* Collaboration, B. Aubert *et al.*, Nucl. Instr. Methods **A479**, 1 (2002).
 [8] *Geant4* Collaboration, CERN-IT-2002-003, submitted to Nucl. Instr. Methods **A**.
 [9] *BABAR* Collaboration, B. Aubert *et al.*, Phys. Rev. D **66**, 032003 (2002).
 [10] *ARGUS* Collaboration, H. Albrecht *et al.*, Phys. Lett. B **185**, 218 (1987); **241**, 278 (1990).
 [11] *Crystal Ball* Collaboration, D. Antreasyan *et al.*, Crystal Ball Note 321 (1983).
 [12] Particle Data Group, K. Hagiwara *et al.*, Phys. Rev. D **66**, 010001 (2002).

TABLE II: Results of the CP likelihood fit, for the full region $-0.4 < \Delta E < 0.4$ GeV and $m_{ES} > 5.2$ GeV/c 2 . Errors are statistical only. The global correlation coefficient is 0.14 for $C_{J/\psi \pi^0}$ and 0.15 for $S_{J/\psi \pi^0}$.

	Fit results
$C_{J/\psi \pi^0}$	0.38 ± 0.41
$S_{J/\psi \pi^0}$	0.05 ± 0.49
Signal ΔE peak position (MeV)	-13.2 ± 7.2
$B^0 \rightarrow J/\psi \pi^0$ signal (events)	40 ± 7
$B^0 \rightarrow J/\psi K_s^0(\pi^0\pi^0)$ background (events)	140 ± 19
Inclusive J/ψ background (events)	109 ± 35
$B\bar{B}$ generic background (events)	52 ± 25
Continuum background (events)	97 ± 22

sive J/ψ and $B\bar{B}$ generic backgrounds each consist of prompt and exponential decay components. Decays appear to be prompt when particles from the reconstructed B are erroneously included in the tagging B vertex. For the $B\bar{B}$ generic background, the prompt and exponential components correspond to the cases where the two decay products forming the J/ψ come from both or just one of the B mesons, respectively. The fraction that is in the exponential component, the decay lifetime parameter, and the resolution parameters are determined from the Monte Carlo simulation.

The Δt PDF for the continuum background has only a prompt component and the resolution parameter values are obtained by fitting the J/ψ_{fake} sample.

The results of the CP asymmetry fit, for all free parameters, are shown in Table II. There are 40 ± 7 signal events in the total sample of 438 selected events. The projection in m_{ES} is shown in Fig. 1. The yields and asymmetry as functions of Δt , overlaid with projections of the likelihood fit results, are shown in Fig. 2. Repeating the fit with the added constraint $C_{J/\psi \pi^0} = 0$ does not significantly change the result for $S_{J/\psi \pi^0}$.

The dominant contributions to the systematic errors in $C_{J/\psi \pi^0}$ and $S_{J/\psi \pi^0}$ are summarized in Table III. The first class of uncertainties are those obtained by variation of the parameters used in the m_{ES} , ΔE , and Δt PDFs, where the dominant sources are the uncertainties in the signal ΔE PDF parameters. A systematic error to account for a correlation between the tails of the signal m_{ES} and ΔE distributions is obtained by using a two-dimensional PDF. Another contribution stems from the impact of EMC energy scale uncertainties on the modeling of the $B^0 \rightarrow J/\psi K_s^0(\pi^0\pi^0)$ background. An additional systematic uncertainty comes from the choice of the binning of the two-dimensional PDFs for the $B^0 \rightarrow J/\psi K_s^0(\pi^0\pi^0)$ and inclusive J/ψ backgrounds.

In summary, an unbinned extended maximum likelihood fit yields 40 ± 7 signal events and the parameters of time-dependent CP asymmetry for the decay $B^0 \rightarrow J/\psi \pi^0$: $C_{J/\psi \pi^0} = 0.38 \pm 0.41$ (stat) ± 0.09 (syst) and $S_{J/\psi \pi^0} = 0.05 \pm 0.49$ (stat) ± 0.16 (syst). Within the

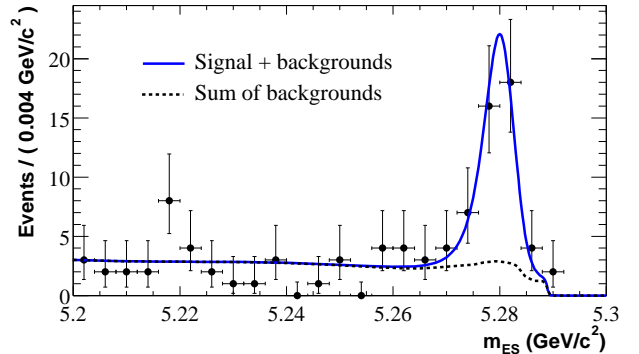


FIG. 1: Projection in m_{ES} for the results of the CP fit, displayed with the added requirement $-0.11 < \Delta E < 0.11$ GeV. In contrast, the CP fit uses the full ΔE region. In the further restricted region $m_{ES} > 5.27$ GeV/c 2 , there are 49 data events (points), of which about 12 events are fit as background. Here, $B^0 \rightarrow J/\psi K_s^0(\pi^0\pi^0)$ and inclusive J/ψ decays contribute to the enhancement in the background distribution at large m_{ES} .

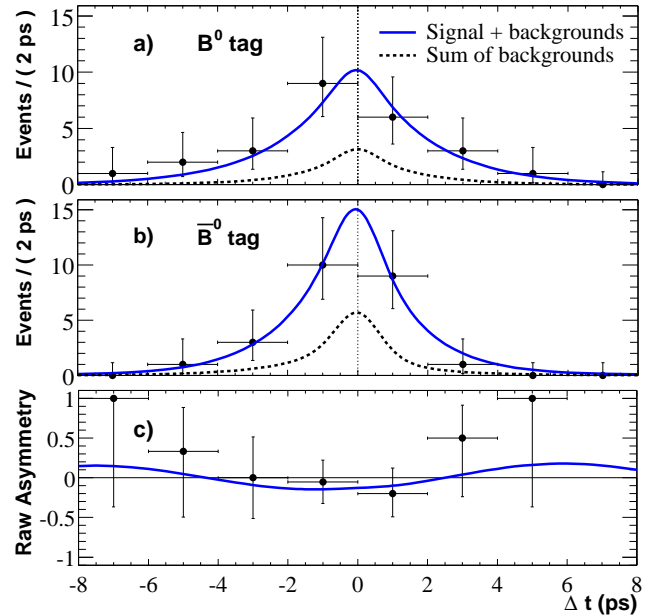


FIG. 2: Distributions of events a) with a B^0 tag (N_{B^0}), b) with a \bar{B}^0 tag ($N_{\bar{B}^0}$), and c) the raw asymmetry ($N_{B^0} - N_{\bar{B}^0}) / (N_{B^0} + N_{\bar{B}^0}$), as functions of Δt . Candidates in these plots are required to satisfy $-0.11 < \Delta E < 0.11$ GeV and $m_{ES} > 5.27$ GeV/c 2 . Of the 49 signal and background events in this region, 25 have a B^0 tag and 24 have a \bar{B}^0 tag, with fit background contributions of approximately 5 and 7 events, respectively. The curves are projections that use the values of the other variables in the likelihood to determine the contributions to the signal and backgrounds.

Standard Model formulation of CP asymmetries, these results demonstrate the possibility, with additional integrated luminosity, of observing penguin contributions in

